PHOTOGRAPH THIS SHEET

AD A109530

DTIC ACCESSION NUMBER

II

LEVEL

INVENTORY

Artifical Icing Test Utility Tactical Transport Aircraft System (UTTAS) Sikorsky YUH-60A Helicopter

Final Rept. Feb. 77

DOCUMENT IDENTIFICATION

USAAEFA Project No. 76-09-1

DISTRIBUTION STATEMENT A

Approved for public release;
Distribution Unlimited

DISTRIBUTION STATEMENT

ACCESSION FOR		
NTIS	GRA&I	☒
DTIC	TAB	☐
UNANNOUNCED		☐
JUSTIFICATION		
BY Per Ltr. on File		
DISTRIBUTION /		
AVAILABILITY CODES		
DIST	AVAIL AND/OR SPECIAL	
A		

DISTRIBUTION STAMP

DTIC
ELECTE
JAN 12 1982
S D
D

DATE ACCESSIONED

81 11 30 134

DATE RECEIVED IN DTIC

PHOTOGRAPH THIS SHEET AND RETURN TO DTIC-DDA-2

DTIC FORM OCT 79 70A

DOCUMENT PROCESSING SHEET

USAAEFA PROJECT NO. 76-09-1

ARTIFICAL ICING TEST
UTILITY TACTICAL TRANSPORT AIRCRAFT SYSTEM (UTTAS)
SIKORSKY YUH-60A HELICOPTER

FINAL REPORT

ROBERT M. BUCKANIN
PROJECT ENGINEER

JOHN S. TULLOCH
CW4, AV
US ARMY
PROJECT OFFICER/PILOT

FEBRUARY 1977

UNITED STATES ARMY AVIATION ENGINEERING FLIGHT ACTIVITY
EDWARDS AIR FORCE BASE, CALIFORNIA 93523

REPORT NUMBER

USAAEFA PROJECT NO. 76-09-1

2. GOVT ACCESSION NO.

AD-A109530

3. RECIPIENT'S CATALOG NUMBER

4. TITLE (and Subtitle)

ARTIFICIAL ICING TEST
UTILITY TACTICAL TRANSPORT
AIRCRAFT SYSTEM (UTTAS)
SIKORSKY YUH-60A HELICOPTER

5. TYPE OF REPORT & PERIOD COVERED

FINAL REPORT
12 October - 3 November 1976

6. PERFORMING ORG. REPORT NUMBER

USAAEFA PROJECT NO. 76-09-1

7. AUTHOR(s)

CW4 JOHN S. TULLOCH
ROBERT M. BUCKANIN

8. CONTRACT OR GRANT NUMBER(s)

9. PERFORMING ORGANIZATION NAME AND ADDRESS

US ARMY AVIATION ENGINEERING FLIGHT ACTIVITY
EDWARDS AIR FORCE BASE, CALIFORNIA 93523

10. PROGRAM ELEMENT, PROJECT, TASK AREA & WORK UNIT NUMBERS

68-U-UA029-01-68-EC

11. CONTROLLING OFFICE NAME AND ADDRESS

US ARMY AVIATION ENGINEERING FLIGHT ACTIVITY
EDWARDS AIR FORCE BASE° CALIFORNIA 93523

12. REPORT DATE

FEBRUARY 1977

13. NUMBER OF PAGES

91

14. MONITORING AGENCY NAME & ADDRESS(if different from Controlling Office)

15. SECURITY CLASS. (of this report)

UNCLASSIFIED

15a. DECLASSIFICATION/DOWNGRADING SCHEDULE

16. DISTRIBUTION STATEMENT (of this Report)

DISTRIBUTION STATEMENT A

Approved for public release;
Distribution Unlimited

17. ... different from Report)

18. SUPPLEMENTARY NOTES

19. KEY WORDS (Continue on reverse side if necessary and identify by block number)

YUH-60A Helicopter (UTTAS)
Prototype Anti-ice/Deice System
Artificial Icing

20. ABSTRACT (Continue on reverse side if necessary and identify by block number)

The United States Army Aviation Engineering Flight Activity, in conjunction with Sikorsky Aircraft Division of United Technologies Corporation, conducted a limited evaluation of the capability of the YUH-60A helicopter equipped with a prototype deice system to fly in a simulated icing environment. Testing was conducted at Fort Wainwright, Alaska, from 12 October through 3 November 1976 and consisted of 9.7 flight hours, of which 3.9 hours were in the icing environment.

~~FOR OFFICIAL USE ONLY~~

(continued)

DD FORM 1 JAN 73 1473 EDITION OF 1 NOV 65 IS OBSOLETE

UNCLASSIFIED

SECURITY CLASSIFICATION OF THIS PAGE (When Data Entered)

20. Abstract

Since Sikorsky Aircraft Division recognized the requirement for rotor blade deice equipment, Sikorsky recommended that no unheated testing be conducted. Although unheated deicing tests were not conducted, it can easily be concluded from these tests that the YUH-60A helicopter does not possess the capability to safely operate in an icing environment without a rotor deice system. Within the scope of this test, the YUH-60A with the prototype anti-ice/deice system displays potential for operating in a moderate icing environment. The six deficiencies found during the test were (1) inadequate deice protection of the main rotor blades, (2) inability to operate the deice system and essential electrical equipment with an AC generator failure, (3) the excessive loss of engine power available with anti-ice system operation, (4) automatic flight control system failures, (5) lack of a system to monitor inlet particle separator turbine operation, and (6) lack of adequate cabin heat at temperatures below -10°C. The six deficiencies noted should be corrected prior to flight in icing conditions. In addition, 14 shortcomings were identified.

[redacted]

USAAEFA PROJECT NO. 76-09-1

ARTIFICAL ICING TEST
UTILITY TACTICAL TRANSPORT AIRCRAFT SYSTEM (UTTAS)
SIKORSKY YUH-60A HELICOPTER

FINAL REPORT

ROBERT M. BUCKANIN
PROJECT ENGINEER

JOHN S. TULLOCH
CW4, AV
US ARMY
PROJECT OFFICER/PILOT

FEBRUARY 1977

UNITED STATES ARMY AVIATION ENGINEERING FLIGHT ACTIVITY
EDWARDS AIR FORCE BASE, CALIFORNIA 93523

[redacted]

DISCLAIMER NOTICE

The findings of this report are not to be construed as an official Department of the Army position unless so designated by other authorized documents.

DISPOSITION INSTRUCTIONS

Destroy this report when it is no longer needed. Do not return it to the originator.

TRADE NAMES

The use of trade names in this report does not constitute an official endorsement or approval of the use of the commercial hardware and software.

UNCLASSIFIED

SECURITY CLASSIFICATION OF THIS PAGE (When Data Entered)

REPORT DOCUMENTATION PAGE

READ INSTRUCTIONS BEFORE COMPLETING FORM

1. REPORT NUMBER: USAAEFA PROJECT NO. 76-09-1	2. GOVT ACCESSION NO.
3. RECIPIENT'S CATALOG NUMBER	
4. TITLE (and Subtitle): ARTIFICIAL ICING TEST UTILITY TACTICAL TRANSPORT AIRCRAFT SYSTEM (UTTAS) SIKORSKY YUH-60A HELICOPTER	5. TYPE OF REPORT & PERIOD COVERED: FINAL REPORT 12 October - 3 November 1976
	6. PERFORMING ORG. REPORT NUMBER: USAAEFA PROJECT NO. 76-09-1
7. AUTHOR(s): CW4 JOHN S. TULLOCH, ROBERT M. BUCKANIN	8. CONTRACT OR GRANT NUMBER(s)
9. PERFORMING ORGANIZATION NAME AND ADDRESS: US ARMY AVIATION ENGINEERING FLIGHT ACTIVITY EDWARDS AIR FORCE BASE, CALIFORNIA 93523	10. PROGRAM ELEMENT, PROJECT, TASK AREA & WORK UNIT NUMBERS: 68-U-UA029-01-68-EC
11. CONTROLLING OFFICE NAME AND ADDRESS: US ARMY AVIATION ENGINEERING FLIGHT ACTIVITY EDWARDS AIR FORCE BASE° CALIFORNIA 93523	12. REPORT DATE: FEBRUARY 1977
	13. NUMBER OF PAGES: 91
14. MONITORING AGENCY NAME & ADDRESS (if different from Controlling Office)	15. SECURITY CLASS. (of this report): UNCLASSIFIED
	15a. DECLASSIFICATION DOWNGRADING SCHEDULE

16. DISTRIBUTION STATEMENT (of this Report)

DISTRIBUTION STATEMENT A

Approved for public release;

Distribution Unlimited

17. ... different from Report)

18. SUPPLEMENTARY NOTES

19. KEY WORDS (Continue on reverse side if necessary and identify by block number)

YUH-60A Helicopter (UTTAS)
Prototype Anti-ice/Deice System
Artificial Icing

20. ABSTRACT (Continue on reverse side if necessary and identify by block number)

The United States Army Aviation Engineering Flight Activity, in conjunction with Sikorsky Aircraft Division of United Technologies Corporation, conducted a limited evaluation of the capability of the YUH-60A helicopter equipped with a prototype deice system to fly in a simulated icing environment. Testing was conducted at Fort Wainwright, Alaska, from 12 October through 3 November 1976 and consisted of 9.7 flight hours, of which 3.9 hours were in the icing environment.

~~FOR OFFICIAL USE ONLY~~

(continued)

DD FORM 1 JAN 73 1473 EDITION OF 1 NOV 65 IS OBSOLETE

UNCLASSIFIED

SECURITY CLASSIFICATION OF THIS PAGE (When Data Entered)

20. Abstract

Since Sikorsky Aircraft Division recognized the requirement for rotor blade deice equipment, Sikorsky recommended that no unheated testing be conducted. Although unheated deicing tests were not conducted, it can easily be concluded from these tests that the YUH-60A helicopter does not possess the capability to safely operate in an icing environment without a rotor deice system. Within the scope of this test, the YUH-60A with the prototype anti-ice/deice system displays potential for operating in a moderate icing environment. The six deficiencies found during the test were (1) inadequate deice protection of the main rotor blades, (2) inability to operate the deice system and essential electrical equipment with an AC generator failure, (3) the excessive loss of engine power available with anti-ice system operation, (4) automatic flight control system failures, (5) lack of a system to monitor inlet particle separator turbine operation, and (6) lack of adequate cabin heat at temperatures below -10°C. The six deficiencies noted should be corrected prior to flight in icing conditions. In addition, 14 shortcomings were identified.

[redacted]

DEPARTMENT OF THE ARMY
HQ, US ARMY AVIATION RESEARCH AND DEVELOPMENT COMMAND
P O BOX 209, ST. LOUIS, MO 63166

DRDAV-EQ

SUBJECT: USAAEFA Project No. 76-09-1, Artificial Icing Test, Utility Tactical Transport Aircraft System (UTTAS), Sikorsky YUH-60A Helicopter, February 1977

SEE DISTRIBUTION

1. The Directorate for Development and Engineering position on USAAEFA's Conclusions and Recommendations are provided herein. Paragraph numbers from the subject report are provided for reference.

a. Paragraph 61: The YUH-60A helicopter does not possess the capability to safely operate continuously in an icing environment approaching the moderate level of intensity or greater without a rotor blade de-ice system. Therefore, this Headquarters has no intention of publishing an Airworthiness Release for the YUH-60A or the UH-60A without a rotor de-icing system installed. The risk of successful qualification of the production rotor de-icing system is considered low. However, additional studies are being performed to insure that the design criteria in terms of liquid water content and partial droplet size are stringent enough to meet moderate icing operational conditions as required by the user.

b. Paragraph 62: The potential was demonstrated, however, greater de-icing coverage of each main rotor blade has been incorporated in the production blade configuration.

c. Paragraph 64a: The insufficient blade coverage of the main rotor blade ice protection system has been corrected for production with greater spanwise and chordwise coverage.

d. Paragraph 64b: This problem has been investigated and the proposed solution is to use the APU generator as a back-up source for the blade de-ice system. An ECP to incorporate this feature is currently being processed.

e. Paragraph 64d: This problem is being corrected in production by changing the AFCS from a fluidic system to an electronic system. The electronic configuration essentially affects the FAS and SAS systems resulting in increased mission performance by utilizing dual 3-axes electronic stabilization versus the single fluidic 3-axes stabilization.

f. Paragraph 64e:

(1) The lack of a system to monitor IPS turbine operation is identified as a deficiency based on:

(a) The engine's susceptibility to FOD without an operable blower.

(b) The requirement to terminate flight in icing conditions if blower was inoperative.

(2) The following points explain why we do not consider this to be a deficiency:

(a) The requirement for termination of flight, if an inoperative blower was indicated, was specifically a conservative test requirement and is not considered valid for production considerations.

(b) No instances of a failed blower of the production configuration has occurred; however, even so, an anti-icing test point was successfully demonstrated with the blower inoperative.

(c) No value of FOD effectiveness with or without a failed blower is known; however, experience with ice ingestion indicated no sizable piece could get through the swirl vanes, past the splitter lip, through the deswirl vanes and IGV without being broken up.

(d) Instances of FOD encountered thus far, blower operative, did not disable an engine beyond some reduced power. The conclusion noted in paragraph 65b will be part of a continuing evaluation, but is not considered imperative until conditions warrant it.

(e) Production maintenance inspection procedures are being established which will include at least a borescope port on the blower.

g. Paragraph 64f: This problem is being corrected in production by changing the heating and ventilation distribution system to be integral with the canopy structure which improves the flow and distribution.

h. Paragraphs 65a, b, and d thru n: Action has been taken to improve or eliminate the shortcoming noted in the production design.

i. Paragraph 65c: We do not agree that this is a shortcoming. Center windshield ice protection was deliberately deleted because of no adverse impact from its non-existence on the CH-47 and S-61 helicopters.

SUBJECT: USAAEFA Project No. 76-09-1, Artificial Icing Test, Utility Tactical Transport Aircraft System (UTTAS), Sikorsky YUH-60A Helicopter, February 1977

Studies at the YUH-60A Preliminary Design Review further indicated that the increased visibility, if it were present, is insignificant in relation to its cost, due to the large offset angle of each crewmember.

j. Paragraph 65j: The absence of a guard may not be a shortcoming, but rather the location close to the maintenance platform. If the guard is provided but is not removed before flight, the detector will not work and then the existence of a guard will be considered a problem. Improved design will be part of the production configuration.

k. Paragraph 68: This WARNING has significant drawback since the purpose of the helicopter is troop assault in which rapid unloading is essential, therefore, it will be applied to peacetime operation only as a CAUTION.

l. Paragraphs 69 thru 71: Action is being taken on each of these three recommendations.

2. Completion of the Maturity Phase of this development/qualification program which includes additional adverse weather testing, should substantiate that the UH-60A can be adequately operated in moderate icing conditions per user requirements.

FOR THE COMMANDER:

Walter A. Ratcliff

WALTER A. RATCLIFF
Colonel, GS
Director of Development
and Engineering

PREFACE

The artificial icing test of the YUH-60A helicopter was conducted jointly by the United States Army Aviation Engineering Flight Activity (USAAEFA) and the Sikorsky Aircraft Division of United Technologies Corporation at Fort Wainwright, Alaska. The test aircraft was maintained by USAAEFA with backup support provided by Sikorsky Aircraft. Aircraft test instrumentation was supplied, calibrated, and maintained by Sikorsky Aircraft personnel. Special acknowledgment is made for the outstanding assistance and support provided at Fort Wainwright by Major James C. Hoodenpyle, CW2 Jefferson R. Watts, and the officers and men of the 222d Aviation Battalion.

Descriptive material on the Normalair-Garrett ice detector system presented in appendix D is used with permission of the company.

TABLE OF CONTENTS

INTRODUCTION

BACKGROUND

1. The United States Army requires an improved operational capability in its utility transport aircraft to satisfy the demand for increased performance and survivability in the mid-intensity combat environment. The utility tactical transport aircraft system (UTTAS) is being developed in response to this requirement and will replace the current utility helicopter in the Army inventory. On 30 August 1972 the United States Army Aviation Systems Command (AVSCOM) awarded a contract to the Sikorsky Aircraft Division of United Technologies Corporation to produce three prototype aircraft and one ground test vehicle. The United States Army Aviation Engineering Flight Activity (USAAEFA) completed an Army Preliminary Evaluation of the Sikorsky YUH-60A in March 1976. A Government Competitive Test (GCT) was completed in September 1976.

2. The UTTAS shall be capable of operation under climatic conditions up to and including moderate icing (ref 1, app A). As a result, USAAEFA was tasked by an AVSCOM test directive (ref 2) to conduct artificial icing tests of the YUH-60A in accordance with the approved test plan (ref 3).

TEST OBJECTIVES

3. The overall test objectives of the UTTAS artificial icing tests were as follows:

a. To provide data to be used for evaluating the ability of the helicopter to effectively operate in a moderate icing environment.

b. To detect and allow for early correction of any aircraft deficiencies or shortcomings.

4. Specific objectives of each testing phase were as follows:

a. Unheated blade phase:

(1) Evaluate the effectiveness of the windshield, pitot-static, engine air induction, and engine anti-ice systems.

(2) Determine the need for additional anti-ice/deice systems.

b. Heated blade phase:

(1) Determine the potential effectiveness of the contractor-provided prototype anti-ice/deice system.

(2) Provide the UTTAS competitors an opportunity to further develop anti-ice/deice systems.

DESCRIPTION

5. The UTTAS is a twin-turbine, single main rotor-configured helicopter capable of transporting cargo, 11 combat troops, and weapons during day, night, visual meteorological conditions (VMC), and instrument meteorological conditions (IMC). Nonretractable wheel-type landing gear are provided. The main and tail rotors are both four-bladed, with a capability of manual main rotor blade and tail pylon folding. A movable horizontal stabilator is located on the tail rotor pylon. A more detailed description of the YUH-60A, serial number 73-21651, is contained in the prime item development specification, operator's manual, and the GCT report (refs 4, 5, and 6, app A). Several modifications were incorporated after the GCT, prior to commencing the icing tests. Since the prototype fluidic stability augmentation system (SAS) gain is temperature-sensitive, heating of the hydraulic fluid was necessary. This was provided by installing an orifice between the pressure and return lines of the No. 2 hydraulic pump. Additionally, the inlets of the sliding access cover were covered to eliminate the flow of cooling air across the SAS servos, and the SAS servos were insulated. The prototype deice system installed on the YUH-60A was designed to provide the capability to deice the main and tail rotor blades. The system incorporated electrothermal heating elements installed on the leading edge of the main and tail rotor blades. The main rotor blade heating elements were installed on the SC 1095 airfoil, not the SC 1095-R8 airfoil used during the GCT. Deice system ON and OFF times were manually set in flight. The YUH-60A also had anti-ice provisions for the pilot and copilot windshields, the pitot-static tubes and their support struts, the engine, and the engine inlets. Appendix B contains a detailed description of the YUH-60A anti-ice and deice systems. A description of the helicopter icing spray system (HISS) installed on a CH-47C helicopter, serial number 68-15814, is presented in references 7 and 8, appendix A, and in appendix C.

TEST SCOPE

6. In-flight artificial icing, utilizing the HISS, was conducted in the vicinity of Fort Wainwright, Alaska, from 12 October through 3 November 1976. A total of 10 icing flights were conducted, totaling 9.7 hours, of which 3.9 hours were in the artificial icing environment. Tests were conducted at gross weights from 14,860 to 16,100 pounds and with longitudinal center-of-gravity (cg) locations from 352.7 to 357.2 inches. Density altitude varied from -1060 to 8960 feet. Icing was accomplished at ambient temperatures from -5.5 to -16.0°C and at liquid water content (LWC) levels of 0.25 gram per cubic meter (gm/m^3) and 0.5 gm/m^3. A summary of icing test conditions is presented in table 1. Icing summaries for each flight are presented in appendix F. The test airspeed in the icing environment was 90 knots true airspeed (KTAS) and main rotor speed was 258 rpm

Table 1. Test Conditions.[1]

Flight Number[2]	Average Gross Weight[3] (lb)	Average Center-of-Gravity Location[4,5] (in.)	Average Density Altitude (ft)	Total Time in Cloud (min)	Average Static Outside Air Temperature (°C)	Programmed Liquid Water Content (gm/m^3)
2	15,600	352.7	340	5	11.0	.25
3	15,700	353.1	2880	10	-5.5	.25
5	16,480	356.3	5180	--	-5.5	---
6	15,900	353.9	5380	16	-5.5	.25
8	16,100	354.8	8960	21	5.5	.25
13	15,560	357.2	450	8	-10.5	.25
14	14,860	354.1	1140	53	-12.0	.25
15	15,180	355.4	720	4	-12.0	.50
16	14,980	354.7	-1060	16	-15.5	.25
17	15,180	355.4	-820	34	-11.0	.50
18	15,420	356.5	9100	--	-15.0	---
19	15,440	356.7	-840	42	-16.0	.25

[1] Configuration: Normal utility; rotor speed: 258 rpm; airspeed in icing cloud: 90 KTAS.
[2] Nonicing flights not presented.
[3] Average gross weight excluding accreted ice.
[4] All longitudinal cg locations were near mid range and exclude the effect of accreted ice.
[5] Average lateral cg: 0.1 inch right.

(98 percent). Flight limitations contained in the operator's manual and the safety-of-flight release (ref 9, app A) were observed during the testing.

TEST METHODOLOGY

7. Artificial icing of the YUH-60A was conducted by flying the test aircraft in a spray cloud generated by the HISS. A detailed discussion of the test sequence and procedures is contained in reference 3, appendix A. Prior to entering the cloud, the test aircraft was stabilized at the predetermined test conditions and base-line trim data were recorded. The test aircraft was then immersed in the spray cloud. After ice accumulation the test aircraft was again stabilized outside the spray cloud at the initial trim airspeed and another data record taken. The ice accretion was then documented by photographic and visual observation. Following data recording, a steady-state autorotation was performed to determine rotor speed degradation with ice accretion. Immersion times were based on pilot judgment, system operation, power required, vibration, visual observations, duration of the HISS water supply, and prior test results.

8. The output from two ice detection systems, one manufactured by Rosemount Engineering Company and one manufactured by Normalair-Garrett Ltd, were used to evaluate icing conditions. A USAAEFA-designed and fabricated visual ice accretion measuring device was used to observe the rate of ice accretion on the airframe. A detailed description of special equipment and instrumentation is provided in appendix D.

9. Test techniques and data analysis methods are presented in appendix E. A Handling Qualities Rating Scale (HQRS), methods used to determine cloud parameters, and definitions of icing types and severities are also presented in appendix E.

RESULTS AND DISCUSSION

GENERAL

10. The evaluation of the capability of the YUH-60A helicopter to operate in an icing environment with anti-ice and prototype main and tail rotor deice systems functioning was conducted using the CH-47C HISS. This evaluation included limited performance and handling qualities investigations following immersion in the spray cloud. Each icing flight was conducted with a contractor engineer controlling the deice system and at no time was the system allowed to operate automatically. Since Sikorsky Aircraft Division recognized the requirement for rotor blade deice equipment, Sikorsky recommended that no unheated testing be conducted (ref 10, app A). Although unheated deicing tests were not conducted, it can easily be concluded from these tests that the YUH-60A helicopter does not possess the capability to safely operate in an icing environment without a rotor deice system. Within the scope of this test, the YUH-60A with the prototype anti-ice/deice system displays potential for operating in a moderate icing environment. The six deficiencies found during the test were (1) inadequate deice protection of the main rotor blades, (2) inability to operate the deice system and essential electrical equipment with an AC generator failure, (3) the excessive loss of engine power available with anti-ice system operation, (4) automatic flight control system (AFCS) failures, (5) lack of a system to monitor inlet particle separator (IPS) turbine operation, and (6) lack of adequate cabin heat at temperatures below -10°C. In addition, 14 shortcomings were identified. The deficiencies identified during these tests should be corrected prior to flight in icing conditions, and the shortcomings should be corrected prior to production.

DEICE SYSTEM OPERATION

General

11. The YUH-60A prototype deice system was evaluated for effectiveness, reliability, maintainability, electrical switching transients, electromagnetic interference (EMI), and electrical power requirements throughout the icing tests. Each icing flight was conducted with the contractor engineer controlling the deice system controller (*ie*, setting ON and OFF times; turning the system ON and OFF), and at no time was the system allowed to operate independently. The main rotor blades tested differed from those used during the GCT in radius, chord, and airfoil section. Test conditions are presented in table 1 and flight summaries for each of the icing test flights are presented in appendix F. During 3.9 hours of flight time in the spray cloud, the deice system was turned on 11 times and cycled 48 times. The only components of the deice system which malfunctioned were the ice detectors. Two separate ice detector problems noted were physical damage to the probe mounted on the No. 2 engine nacelle and freeze-up of the probe

mounted on the No. 1 engine nacelle. Electrical problems resulting from deice system activation were encountered and partially solved during the testing.

Electrical Malfunctions

12. Unpredictable electrical malfunctions of the AFCS occurred throughout the icing tests. The most serious malfunction was a left lateral runaway trim the second time the deice system was turned on. Right lateral cyclic was immediately applied to stop the left roll, as lateral control force increased to approximately 8 pounds (HQRS 8). Eight pounds of control force is the limit of the force augmentation system (FAS) in the lateral axis. Recycling the FAS and flight path stabilization (FPS) controls did not eliminate the runaway trim condition, and after approximately 10 minutes the left lateral force slowly decreased to zero. This was followed by a gradual build-up to approximately 8 pounds right lateral force. Pulling the electronics-cooling circuit breaker eliminated the lateral trim runaway. The most probable cause of the lateral trim runaway was the electrical switching transients that took place when the deice system was turned on. A temporary procedure was devised whereby the FAS circuit breaker was pulled and the FAS/TRIM and FPS controls were deactivated prior to turning the deice system on. The FAS/TRIM and FPS controls were then reactivated and the FAS circuit breaker pushed in once the deice system was ON. This procedure reduced the number of AFCS malfunctions. The last AFCS malfunction occurred late in the program, when a FAS failure occurred. The FAS failure was corrected by resetting the FAS controls and the flight continued. The AFCS failures experienced throughout the test are a deficiency.

Ice Detector Malfunctions

13. Three separate malfunctions of the Rosemount ice detectors were noted during the tests. The malfunctions were physical damage to the ice detector probe mounted on the No. 2 engine nacelle; freeze-up of the ice detector probe mounted on the No. 1 engine nacelle (photo 1, app H); also, erroneous ICE-DETECTED indications were present when the fairing heater for the tail cone-mounted tail rotor camera was turned on. Since the heated camera fairing was part of the special instrumentation, the EMI associated with its operation is not considered a problem; however, the presence of EMI does indicate that EMI shielding will be needed when electrical components that use large quantities of electrical power are installed.

14. Data analysis after flight 13 revealed that the Rosemount ice detector probe mounted on the No. 2 engine nacelle had malfunctioned throughout the flight. Inspection of the icing probe by a Rosemount technical representative revealed that the probe had been bent. Photo 2, appendix H, shows the location of the icing probe relative to the fold-out work platform that is part of the engine cowling. Although not confirmed, the probe could have inadvertently been bent during maintenance, since the probe is about knee height as one steps from the treadway in front of the engine intake to and from the work platform. The damaged ice

detector was replaced and a removable guard was installed any time the aircraft was not flying. The absence of a guard to protect the delicate icing probe is a shortcoming.

15. After flight 16, visual inspection of the aspirated Rosemount ice detector probe mounted on the No. 1 engine nacelle (photo 1, app H) revealed that the probe had frozen over. A continuity check was made of the heater element circuit, and a broken wire was discovered. The broken wire was repaired and no additional probe freeze-up occurred.

Electrical Power Requirements

16. Representative electrical power requirement data and other pertinent information relative to deice system operation are presented in table 2. Since the main and tail rotor heater zones function independently, the peak electrical load could be the sum of the main and tail rotor electrical loads. The largest combined electrical load was 33.3 kilovolt-amperes (kVA), which is 33 percent higher than the contractor estimate of 25 kVA. The 33.3 kVA electrical power requirement is 88 percent of the maximum continuous generator rating (38 kVA). Within the scope of this test, the electrical power demand of the deice system did not exceed the capability of a single AC generator.

17. The prototype deice system is designed to operate from the electrical power of one aircraft AC generator. The No. 2 AC generator is dedicated to the deice system when the deice system is turned on by electrically switching to the No. 1 AC generator the electrical load normally carried by the No. 2 AC generator. This design does not allow for deice system operation if either AC generator fails. In the case of the No. 2 AC generator failing, the deice system is deprived of electrical power, since no alternate source is provided. In the case of the No. 1 AC generator failing, the deice system is automatically turned off, and the aircraft's AC electrical load is transferred to the No. 2 AC generator. The inability to operate the deice system and essential electrical equipment after an AC generator failure is a deficiency.

Maintainability

18. During the icing tests, troubleshooting and system checkout of the prototype deice system was facilitated by the "bread board" design of the system controller. Although no deice system failures occurred, malfunctions of the deice system would have been easily detected and isolated by simply watching the indicators on the deicing engineer control panel. Two amber malfunction lights (main rotor failure, tail rotor failure) were provided on the systems control panel for fault detection. The malfunction lights would not provide adequate fault isolation information for maintenance purposes. Maintenance time in the field will be greatly reduced if adequate fault isolation is incorporated in the deice system. The lack of adequate fault isolation will degrade system maintainability and is a shortcoming.

Table 2. Electrical Power Required.

Flight Number	Average Static Outside Air Temperature (°C)	Programmed Liquid Water Content (gm/m3)	Total Time in Cloud (min)	Main Rotor Deice System		Tail Rotor Deice System		Peak Electrical Power	
				ON Time (sec)	OFF Time (sec)	ON Time (sec)	OFF Time (sec)	Main Rotor (kVA)	Tail Rotor (kVA)
14	-12.0	.25	53	19	236	7	93	28.0	5.3
17	-11.0	.50	34	20	180	8	69	27.1	5.2
19	-16.0	.25	42	22	236	13	93	27.4	5.2

ANTI-ICE SYSTEMS OPERATION

General

19. The anti-ice systems of the YUH-60A were continuously evaluated for effectiveness, reliability, maintainability, electrical power requirements, and bleed air requirements throughout the icing tests. During the 3.9 hours of flight time in the spray cloud, the anti-ice systems provided adequate ice protection except for the pilot windshield, windshield wiper drive cable, and windshield wiper motor. Components changed during the test included the pilot windshield anti-ice controller, two windshield wiper drive cables for the pilot windshield wiper, and a windshield wiper motor. Except for the components noted, no adverse reliability or maintainability characteristics of the various components of the anti-ice systems were observed.

Engine

20. Engine anti-icing was accomplished by a combination of hot axial compressor discharge air and heat transfer from the air/oil cooler in the engine frame. The system was controlled by the ENG ANTI-ICE switch located on the overhead switch panel. A detailed description of the system is presented in appendix B. During the testing the system operated without any failures and with no unscheduled maintenance being required. Within the scope of this test, the engine anti-ice system is satisfactory.

Engine Inlet

21. The engine inlet was heated by hot engine bleed air. A system description is presented in appendix B. The system operated with no failures and no ice accumulation was observed on the inlets. Within the scope of this test, operation of the engine inlet anti-ice system is satisfactory.

Windshield

22. The pilot windshield anti-ice failed during two flights. After the first windshield anti-ice failure the pilot windshield anti-ice temperature controller was replaced. Postflight inspection after the second failure revealed that the pilot windshield had not been properly manufactured. The windshield design specified that the temperature sensors (two) be placed at the top inside corner and at the bottom outside corner of the windshield. The diagonal placement of the sensors allows for temperature averaging in the windshield anti-ice controller, and is done to account for the difference in windshield width, top and bottom, which has a direct influence on the electrical power necessary to anti-ice the windshield. The temperature sensors embedded in the pilot windshield were both installed along the top edge, which resulted in insufficient electrical power being supplied to anti-ice the windshield. Correction of this problem resulted in satisfactory

windshield anti-ice protection for the remainder of the icing tests. The copilot windshield was properly manufactured. The improper manufacture of the pilot windshield is a shortcoming.

Windshield Wiper Drive Cable

23. The pilot windshield wiper drive cable malfunctioned on four occasions. The cause of the malfunction was the inner drive cable shortening as increased torque was applied to the wiper blade, when it increased in weight due to ice accretion. Visual inspection of the pilot windshield wiper drive train revealed evidence of the driven end sliding out of the driving end at the windshield wiper motor connection. Several new cables were installed, and each exhibited the same characteristics. A drive cable of sufficient length was locally manufactured, installed, and operated satisfactorily. The inability of the windshield wiper drive cable to withstand the torque necessary to drive the windshield wiper with ice accreted is a shortcoming.

INLET PARTICLE SEPARATOR

24. Ice particles of undetermined size were observed entering the engine inlets; however, there was no foreign object damage (FOD) to the engine compressor. An IPS on each engine is designed to protect the engine from FOD (ref 5, app A). Without an operable IPS the engine is very susceptible to FOD, especially in an icing environment. Failure of either IPS during the icing tests would have required termination of flight in icing conditions. For this reason, a special IPS differential pressure gauge was installed in the cockpit to monitor IPS operation. The production aircraft should incorporate a system to monitor IPS operation. The lack of a system to monitor IPS turbine operation is a deficiency.

FLIGHT CONTROL SURFACE ICE ACCRETION AND SHEDDING CHARACTERISTICS

General

25. Flight control surface ice accretion and shedding characteristics were documented by in-flight visual observation, high-speed motion picture photography, postflight measurements, and still photography. The effects of ice accretion and shedding on performance were quantitatively evaluated prior to, during, and after each spray cloud immersion flight and are discussed in paragraphs 43 through 49. Flight control surfaces are defined as the stabilator and the main and tail rotors, including the rotating components that were exposed to the free stream.

Main Rotor Blades

26. The main rotor deiced blades all showed the same ice accretion and shedding characteristics. At the end of the flights of longest immersion for each test condition, the protected areas (35 to 95 percent spanwise; 8 and 12 percent chordwise top and bottom, respectively) were clear of ice and there was no evidence of runback on either side of the blade. There was, however, a large ice buildup on the inboard unprotected portion of the blade, and a significant buildup aft of the protected area on the bottom side of the blade out to approximately 60 percent span. Following a 34-minute immersion at -10°C and LWC of 0.5 gm/m^3 (flight 17), ice thickness was 1 inch on the leading edge at 15 percent span. During the flight, ice accreted as a solid mass on the unprotected leading edge and wrapped around the leading edge from approximately 10 percent chord, top side, to approximately 20 percent chord on the bottom side. Aft of the solid wrap-around ice in the unprotected area, there was "stalk" ice on both top and bottom of the blade. (Stalk ice is defined as ice that forms slender irregular shaped rods of ice, generally into the direction of the local airflow.) The amount observed on the top side of the blade was sparsely located; however, the stalk ice formation extended to the trailing edge on the bottom side of the blade out to approximately 60 percent span (photo 3, app H). Discontinuities on the bottom side of the blade, such as the boron strip near the trailing edge, showed a pronounced affinity for ice accretion. This accretion pattern was typical for all three of the long immersion flights. Future designs should consider increased chordwise ice protection on the main rotor blade.

27. Discussions concerning shedding characteristics must be qualified as to whether the shed was natural or induced and also the area from which the ice was shed. (Natural shedding is defined as shedding caused by the accreted ice severing its bond with the surface to which it is attached without pilot-induced influences such as changes in rotor speed and/or flight control inputs.) With the deice system operating, the protected portion of the blade controlled the ice accretion and produced a symmetrical shedding. Visual observation and high-speed motion pictures revealed that the shedding occurred at random blade azimuth positions, making it impossible to predict ice trajectory. At times the shed ice was struck by the following blade, and shattered into smaller particles. Visual inspection of the main rotor blades after each flight revealed no damage to the blades other than an occasional paint chip. The crew heard ice strike the airframe and observed ice striking the windshield; however, visual inspection revealed no damage to either. The remainder of the shed ice seemed to drop away with little or no horizontal velocity imparted due to blade rotation. The engines were borescoped after each icing test flight. The results of the borescope observations revealed no FOD to the compressors, even though ice was observed and photographed entering the engine inlets. Within the scope of this test, the ice shedding characteristics of the protected portion of the main rotor blades with the deice system operating were satisfactory.

28. The stalk ice that accreted on the bottom side of the main rotor blade showed no tendency to shed, either naturally or as a result of a rotor speed sweep. The solid wrap-around ice attached to the unprotected inboard portion of the leading edge did shed both naturally and as a result of rotor speed sweeps. Natural shedding was characterized by a momentary increase in lateral vibrations at the pilot seat, coupled with a reduction in the engine power required to remain in the icing environment. During a 39-minute immersion at -11°C and 0.5 gm/m^3 LWC (flight 17), 1 inch of ice accreted on the leading edge out to 14 percent span, and then 1/4 inch of ice accreted from 14 to 17 percent span, indicating that a natural shed occurred. A rotor speed sweep was also accomplished during this flight after postcloud trim data were recorded by beeping the rotor to 105 percent and then immediately beeping to 98 percent. Lateral vibrations similar to those present during the ice cloud immersion were felt during the rotor speed sweep. Trim data recorded afterwards revealed a significant reduction in power required. The postcloud average torque reading was 57 percent, which dropped to 45 percent following the rotor speed sweep. A rotor speed sweep was also accomplished after postcloud trim data were recorded on a 44-minute flight at -16°C and 0.25 gm/m^3 LWC (flight 19) in which the induced shed was not symmetrical and a very uncomfortable 0.15g 1-per-rotor-revolution (1/rev) lateral vibration was recorded from the Chadwick-Helimuth vibration meter. Several additional rotor sweeps failed to eliminate the asymmetric condition and therefore a rotor speed sweep is not a satisfactory means of shedding ice from the inboard portion of the blade, since it was not always successful. The inadequate ice protection of the main rotor blades is a deficiency which is further discussed in paragraph 45.

29. At the conclusion of each icing flight a running landing, using minimum control inputs, was executed to retain as much accreted ice as possible. A remote area was selected to prevent injury to personnel or damage to structures, since large pieces of ice (1 by 1 by 3 inches) were slung up to 75 yards from the aircraft when the engines were shut down. The following WARNING should be placed in the operator's manual:

WARNING

Following flight into icing conditions, ice shed from the rotor blades and/or other rotating components presents a hazard to personnel during ground operation and shutdown of the helicopter. Ground personnel should remain well clear of the helicopter during landing, ground operation, and shutdown. Passengers/crewmembers should not exit the helicopter until the rotor has stopped.

Main Rotor Hub

30. Visual inspection of the main rotor hub area after each icing flight revealed symmetrical ice accretion on similar components with no evidence of any shedding. The amount of ice accreted depended on location, with the components on the top accreting more ice than those on the bottom. Photo 4 (app H) from flight 19 is a typical example of what was observed after each long immersion flight. During this flight the thickness of the ice on the bifilar weights was 1/2 inch. Each weight had complete freedom of movement. There were no apparent changes in vibration levels attributed to ice accretion on the bifilar weights. The remainder of the moving components in the hub area, such as droop stops, pitch change rod ends, lag dampers, and elastomeric bearings, are somewhat protected and showed no indication of accreting enough ice to impair movement. On two occasions the droop stop on the instrumented blade remained extended and did not retract on shutdown. This discrepancy was attributed to a weak spring and not to ice accretion. Within the scope of this evaluation, ice protection is not required in the hub area.

Main Rotor Pitch Change Links

31. Photo 4, appendix H, shows a bulbous ice accretion on the lower end of the pitch change link which was typical for all icing flights. There was no evidence of interference between the ice and the airframe or that interference would occur with ice growth during longer flights. Loads in the pitch change links were recorded and no significant increase in loads as a function of ice accretion on the links or the rotor blades was noted. Within the scope of this test, ice protection for the pitch change links is not required.

Tail Rotor

32. Visual inspection of the tail rotor after each icing flight revealed ice on all components of the tail rotor. Accretion patterns on each tail rotor blade were the same. The accretion patterns on each pitch change link were also the same. The remaining components of the tail rotor all accreted ice; however, like the blades and pitch change links, the ice thickness was always less than the ice accreted on the vertical fin. Photo 5, appendix H, is representative of what was observed following each long immersion flight, with the exception of one flight where the deice system cycle times were not optimized. Some evidence of localized natural shedding was seen (photo 5) at about 30 percent span; however, it appeared to be a function of flexing in that area, and was never observed to have progressed beyond 40 percent span. Ice trajectory as a result of deice system operation or natural shed was not determined photographically; however, visual inspection of the airframe revealed no damage.

33. Films taken from the chase aircraft indicate that the exhaust plume from the HISS is deflected downward in the area of the top half of the tail rotor disc. There could also be some heating of the tail rotor by the UTTAS exhaust plumes. Attempts to determine if the exhaust plumes were heating the tail rotor were unsuccessful using the imbedded temperature sensors in the tail rotor. Films also

show that the top 40 percent of the tail rotor disc is not in the spray cloud when the main rotor is centered vertically in the spray cloud. Further tests should be accomplished with the tail rotor fully immersed in the spray cloud and with infrared countermeasure devices installed.

Stabilator

34. Visual inspection of the stabilator after each icing flight revealed different accretion patterns for the right and left sides, as can be seen in figure A. The dimensions and ice description that accompany figure A are representative of the data recorded after each of the long immersion flights. The clear ice along the inboard leading edge on the left side suggests that the engine exhaust is influencing accretion patterns in that area. Ice accreted on the inboard end did not restrict stabilator movement; however, any change in exhaust gas flow due to the installation of infrared countermeasure devices will require reevaluation of the accretion characteristics. Evidence of a natural shedding was only observed on the right stabilator tip, and occurred outboard of the splice (fig. A). Qualitatively, handling qualities were unaltered due to ice accretion on the stabilator.

AIRFRAME ICE ACCRETION AND SHEDDING CHARACTERISTICS

General

35. Airframe ice accretion and shedding characteristics were documented by in-flight visual observation, high-speed motion picture photography, postflight measurements, and still photography. Generally, each flight revealed that ice would accrete on any unprotected portion of the airframe exposed to the free stream, as seen in photo 6, appendix H. Postflight measurements of ice accretion on various airframe components are presented in appendix F (icing flight summaries). Only those components displaying significant accretion and/or shedding characteristics are discussed in this section.

Windshield Frames

36. Visual inspection of the windshield frames after each icing flight revealed a scalloped accumulation of ice at the top and outside edge of both the pilot and copilot windshields (photo 7, app H). The scalloped accumulations were caused by ice particles melting on the heated windshield and then flowing to the windshield frame and refreezing. Accumulations of 1 inch were common after 30 minutes in the spray cloud and there was no natural shedding observed during the test. The potential for engine FOD does exist, since the engine inlets are above and behind the windshield frames. During autorotation the scalloped ice accretion disrupted the airflow to the pitot-static tubes and at times caused a 10-knot difference between the pilot and copilot airspeed indicators. In one case, while recording postcloud autorotation data, the airspeed difference was sufficient to cause a stabilator shutdown, which reverted the stabilator to a manual mode of operation. The stabilator was reset to the automatic mode of operation once the

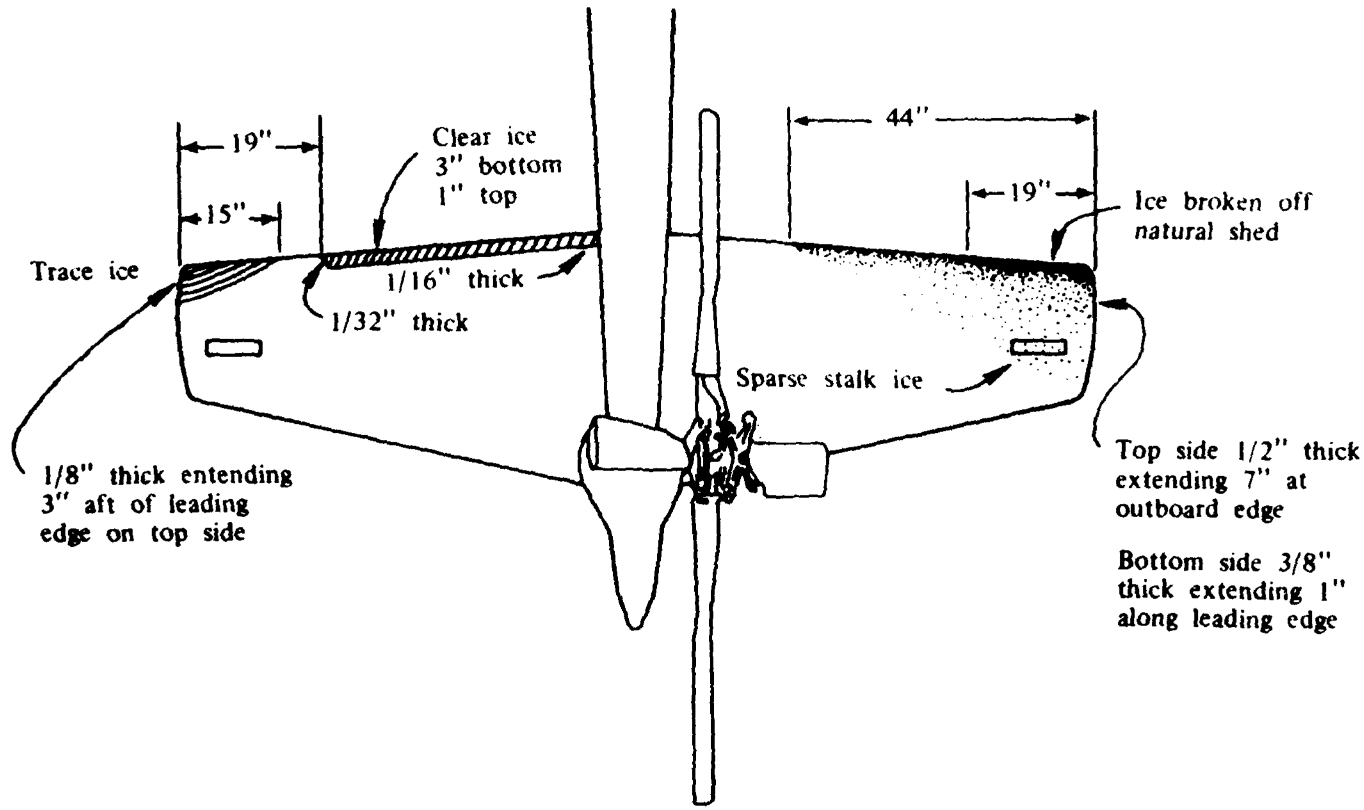

Figure A. Stabilator Ice Accretion Characteristics.

aircraft regained straight and level flight. The large accumulation of ice on the pilot and copilot windshield frames could cause engine and/or airframe FOD and is a shortcoming.

Center Windshield

37. The center windshield has no ice protection and iced over immediately upon entering the spray cloud. Ice thickness measurements for the individual icing flights are recorded in the icing flight summaries presented in appendix F. The pilot and copilot fields of view are restricted after an icing encounter, and would hamper the crew's ability to visually acquire the runway environment after breaking clear of clouds during an instrument approach. Additionally, circling instrument approaches will be more difficult to execute when combining the restricted field of view with reduced visibility. Tactical operations that require flight in icing conditions, an instrument approach, and then nap-of-the-earth (NOE) flight to a landing zone will be difficult to execute. Shedding was not observed during the test; however, the potential for engine FOD does exist, as described in paragraph 36. The lack of ice protection on the center windshield is a shortcoming.

Windshield Wiper

38. Typical ice accretion on the windshield wiper is shown in photo 8, appendix H. Ice thickness measurements for the individual icing flights are recorded on the icing flight summaries presented in appendix F. Photo 7 was made after a 39-minute flight at -11°C and 0.5 gm/m^3 LWC (flight 17) and shows a thick accretion of ice on the wiper blade, lesser amounts accreted on the wiper arms, and some natural shedding. The greater ice accumulation on the wiper blade was caused by the moisture from the melted ice particles refreezing as the wiper blade passed across the windshield. Some natural shedding from the wiper blade was observed on other icing flights, but was not predictable. During this same flight, the wiper motor stalled several times and finally overheated after 27 minutes in the spray cloud. The inability of the windshield wiper motor to drive the windshield wiper with a large accumulation of ice is a shortcoming.

Pilot Doorframe

39. Ice accumulated in the crack between the pilot door and the doorframe because of the melted ice that flowed from the windshield. Photo 8, appendix H, shows the entire doorframe adjacent to the windshield iced over. The ice penetrated the crack between the door and doorframe, forming a bond that made it impossible to jettison the door using only the emergency door release. Pushing on the door was inadequate to break the bond. Striking the door was ineffective because there was no convenient solid door structure. The ice bond was broken when the door handle was used. Although ice build-up was observed along the copilot door, the moisture had not frozen between the door and doorframe. The door was jettisoned by pulling the emergency release handle and striking the door firmly. All icing tests were flown at 90 KTAS with an inherent sideslip of 5 degrees right which resulted in the ice accreting in the pilot doorframe. Icing flights at airspeeds where

inherent sideslip is left would most likely result in similar ice accretion patterns on the copilot door. The inability to jettison the pilot door with ice accreted on the doorframe, using the emergency release, is a shortcoming.

Pitot-Static Tube Support Strut

40. The pitot-static tube support strut is mounted on a 1/2-inch-high unheated mounting pad directly in front of the engine inlet. After a 39-minute flight at -11°C and 0.5 gm/m^3 LWC (flight 17), a small accumulation of ice was observed aft of the mounting pad (photo 7, app H), forming an ice bridge between the skin of the aircraft and the unheated base of the support strut. Similar ice accretion was observed after flight 15. No natural shedding was known to have occurred; however, the potential for engine FOD does exist should natural shedding occur. The presence of accreted ice directly in front of the engine inlet aft of the pitot-static tube support strut is a shortcoming.

Engine Nacelle

41. Ice accretion patterns around the engine nacelle, similar to that shown in photo 2, appendix H, were observed after each icing flight. The amount accreted varied as a function of time and there was no evidence of natural shedding. Ice also accreted on the wiring and fire extinguisher discharge tube just inside the engine cooling air inlet. The presence of ice and moisture within the engine nacelle is a potential electrical problem, and proper protection should be provided for all moisture-intolerant components in the engine nacelle.

42. The engine nacelle skin immediately ahead of the ice detectors accreted ice. Photos 1 and 9, appendix H, show the aspirated Rosemount ice detector mounted on the No. 1 engine nacelle after 16- and 44-minute flights at -16°C and 0.25 gm/m^3 LWC, respectively, and are representative of the ice growth immediately ahead of the detector. To provide accurate information to activate the deice system (AUTO mode), the ice detector should be in undisturbed free stream air. The ice accreted immediately ahead of the ice detector will adversely influence operation of the ice detector and is a shortcoming.

PERFORMANCE

Level Flight

43. A limited level flight evaluation of the YUH-60A helicopter was conducted at the test conditions shown in table 1. The level flight performance data were obtained from pre- and postcloud test data. A summary of the individual test results is shown in table 3. The power required for level flight increased after flight in the icing environment at the same trim airspeed. The major cause of the large increase in power required for level flight was attributed to ice accumulation on the inboard sections of the main rotor.

Table 3. Level Flight Performance.[1]

Flight Number	Average Static Outside Air Temperature (°C)	Programmed Liquid Water Content (gm/m3)	Total Time in Cloud (min)	Average Density Altitude (ft)	Gross Weight		Engine Power Required	
					Precloud (lb)	Postcloud[2] (lb)	Precloud (shp)	Postcloud[3] (shp)
Deice System OFF								
2	-11.0	.25	5	340	15,630	15,530	1151	1284
3	-5.5	.25	10	3340	15,810	15,590	1199	1267
15	-12.0	.50	4	960	15,280	15,060	1107	1683
Deice System ON								
6	-5.5	.25	8	5300	15,870	15,790	1093	1457
8	-5.5	.25	7	8980	16,390	16,170	1156	1353
13	-10.5	.25	8	920	15,670	15,470	1024	1424
14	-12.0	.25	53	1640	15,220	14,510	1159	1684
16	-15.5	.25	16	-880	15,200	14,830	1159	1515
17	-11.0	.50	34	-320	15,850	15,040	1097	1419
19	-16.0	.25	42	-380	15,730	14,630	1224	1526

[1]Trim airspeed: 90 KTAS; rotor speed: 258 rpm.
[2]Postcloud gross weight does not include weight of accumulated ice.
[3]Postcloud power-required data are affected by ice shedding characteristics. See general comments section of icing flight summaries in appendix F.

44. The level flight performance tests without the deice system operating were limited to flights that determined deice system OFF times. Significant increases in power required for level flight were encountered after only a few minutes exposure to the icing environment. Insufficient data precluded precise assessment of the test helicopter's capability for continuous flight in icing conditions.

45. The power required for level flight during the heated phase tests also showed a significant increase with the accumulation of ice on the aircraft. The additional power required ranged from 15 to 31 percent of the precloud trim point. On flight 8 in programmed 0.25 gm/m^3 LWC and -5°C, the icing cloud was entered with a power-available margin of 24 percent. After 7 minutes, continued flight in the cloud was not possible because of insufficient power. Repeated attempts to reenter and remain in the icing cloud were unsuccessful. On flight 17 (programmed 0.5 gm/m^3 LWC and -11°C), after the postcloud performance tests were completed, a rotor speed sweep to 105 percent was conducted in an attempt to shed the ice remaining on the inboard section of the main rotor. Shedding was observed during the rotor speed sweep and as a result, the power required for level flight decreased to approximately half of the total power increase from the precloud trim point. In-flight motion picture film and postflight inspection confirmed that ice was shed from the main rotor blades, inboard of the heated portion (zero to 35 percent span). This indicated that a large portion of the increase in level flight power required was due to the ice remaining on the leading edge of the unprotected inboard section of the main rotor blade. The inadequate ice protection of the main rotor blades is a deficiency.

<u>Power Loss With Anti-Ice Systems</u>

46. Engine performance tests were conducted to quantify the power-available losses due to engine and engine inlet anti-ice systems. Tests included flight with both systems OFF for base-line data; with engine-only anti-ice ON; and with both systems ON. Pitot head, windshield anti-ice systems, and cabin heat remained on during all these tests. Test results are shown in figures 1 and 2, appendix G.

47. Dual-engine power available was reduced by 685 shp due to the engine and engine inlet anti-ice systems operation. The engine anti-ice system contributed 69 percent of the total power-available loss and the engine inlet anti-ice system contributed the remaining 31 percent. The No. 1 and No. 2 engines contributed 360 and 325 shp, respectively, to the power-available loss. This power-available loss was based on turbine inlet temperature, which was the limiting engine parameter at the test conditions flown. The excessive loss of engine power available with anti-ice system operation is a deficiency.

<u>Autorotational Descent</u>

48. Autorotational descent performance was evaluated at the conditions shown in table 1. Test techniques are discussed in appendix E. Pilot qualitative comments regarding changes in autorotational characteristics due to ice accumulation are

presented in the general comments section of appendix F. Table 4 is a summary of the autorotational descent performance during the icing tests.

49. The pre- and postcloud data presented in table 4 show that a decrease in autorotational descent performance occurred with ice accumulation on the main rotor blades. The test results with clean blades and blades with ice accumulated are difficult to compare because of the gross weight, density altitude, and collective control position changes and lack of sufficient base-line autorotational data with the heated rotor blades. After a 53-minute flight at -12°C and 0.25 gm/m^3 LWC (flight 14), the stabilized autorotational rotor speed was at the minimum power-off continuous rotor speed limit of 95 percent with the collective control full-down. The maximum continuous power-off rotor speed allowed by the safety-of-flight release was 105 percent. On flights 17 and 19 the ship's system airspeed indicator fluctuated ±5 knots while in the stabilized autorotation. This fluctuation was attributed to the turbulent airflow caused by the buildup of ice at the top of the windshields in front of the pitot-static probes (para 36). Within the scope of this test, autorotational descent performance as a result of ice accumulation was degraded.

VIBRATION

50. Vibration characteristics were qualitatively and quantitatively assessed throughout the flight tests. Accelerometers were mounted on the pilot seat pan, the main transmission, the tail rotor gearbox, and at the aircraft cg. Qualitative comments are included in the general comments section of the icing flight summaries in appendix F. Generally, the main rotor 1/rev and 4/rev vibration levels remained unchanged after flight in the icing environment. While in the cloud, the main rotor 1/rev and 4/rev vibrations increased slightly at the pilot seat and aircraft cg in all axes. These increases in vibration levels were normally associated with ice shedding from the main rotor during and after a deice system heating cycle or a natural shed. The increased vibrations were not uncomfortable to the crew. There were no significant changes in the main transmission or tail rotor gearbox vibration levels.

51. A rotor speed sweep to 105 percent was conducted during a flight at -16°C and 0.25 gm/m^3 LWC just after a deice heating cycle (after approximately 30 minutes in the cloud) in an attempt to shed the ice remaining on the inboard section of the main rotor. Additional ice was shed from the main rotor; however, it was not shed symmetrically. This asymmetrical shed of ice caused a significant increase in the main rotor 1/rev vibration level in all axes. The 1/rev vibration at the pilot seat in the lateral axis was predominant. It increased from 0.05g just before the rotor speed sweep to 0.12g. This level of vibration at the main rotor 1/rev frequency was very uncomfortable to the pilot and copilot. The 1/rev vibration on the vertical axis was predominant at the aircraft cg. Vibration characteristics at this condition are shown in figures 3 and 4, appendix G. Figure 3 shows the normal vibration characteristics of the helicopter at the pilot

Table 4. Autorotational Descent Performance.[1]

Flight Number	Average Static Outside Air Temperature (°C)	Programmed Liquid Water Content (gm/m^3)	Total Time in Cloud (min)	Average Density Altitude (ft)	Collective Control Position[2] (%)	Maximum Stabilized Rotor Speed (%)	Rate of Descent (ft/min)	Average Gross Weight (lb)
14[3]	-12.0	.25	Zero	Zero	Zero	105	3250	15,820
			53	-80	Zero	95	2800	14,600
17[4]	-11.0	.50	Zero	-1280	7	104	3250	15,300
			34	-1460	Zero	103	3300	14,970
19[4]	-16.0	.25	Zero	-580	7	104	3200	15,280
			42	-700	Zero	97	4000	14,480

[1]Trim airspeed: 72 KCAS.
Deice system ON.
[2]Measured from full-down.
[3]Collective rigging adjusted after flight 14 (equivalent to approximately 8 percent).
[4]Airspeed indication fluctuated ±5 knots during autorotation.

seat without ice accumulation and figure 4 shows the vibration increase resulting from the asymmetrical shed.

HUMAN FACTORS

Cabin Heater

52. The cabin heater was qualitatively evaluated throughout the testing and was found inadequate for passenger and crew comfort at -10°C and below. Cabin temperature data were not recorded; however, qualitative comments were made during flight when the cabin heater was ON and the cabin temperature selector was at the maximum heat position. The flight test engineer at fuselage station (FS) 351 wore long woolen underwear, a heavy flannel shirt, corduroy trousers, a ZWU-1/P winter flight suit, and cold weather mukluks, and reported inadequate cabin heating. In addition to heavy winter clothing, the flight test engineer at FS 288 wore Nomex flight gloves and reported difficulty in manually recording data due to cold hands and loss of feeling in the fingers. The pilot and copilot also wore heavy winter clothing and insulated boots, and experienced cold feet and some loss of feeling in the toes. The lack of adequate cabin heat at temperatures below -10°C is a deficiency.

Caution/Advisory Panel

53. An ICE DETECTED word segment is provided on the caution/advisory panel that receives its signal from the Rosemount ice detector mounted on the No. 1 engine nacelle. The ICE DETECTED word segment would illuminate intermittently when the helicopter was immersed in the cloud and on numerous occasions illuminated when flying in clean air. Since illumination of a caution/advisory word segment also illuminates the MASTER CAUTION, the pilot continually has his attention directed to the caution/advisory panel. This diversion of attention increased pilot workload, added psychological stress, and resulted in loss of confidence in the caution/advisory panel. The erroneous intermittent illumination of the ICE DETECTED word segment on the caution/advisory panel is a shortcoming.

54. The amber MASTER CAUTION light and the amber ICE DETECTED word segment that illuminate when ice is detected are not in accordance with the identification color specified in military specification MIL-C-25050 (dated 29 October 1954). Since the detection of ice does not indicate impending danger requiring extreme caution, the MASTER CAUTION light should not illuminate when ice is detected, and the ICE DETECTED word segment should be moved to the advisory section of the caution/advisory panel.

Deice System Failure Lights

55. The deice system failure lights are on the blade deice control panel which is located on the left rear portion of the lower console. Both the main and tail rotor failure lights are amber and are completely out of the pilot's normal field of view. The only method available to the pilot to detect a system failure is to turn the head and look at the failure lights. Such head and eye movement during flight in IMC is conducive to spatial disorientation. The placement of the deice system failure lights out of the pilot's field of view is a shortcoming.

Icing Severity Indicator

56. No cockpit indication of icing severity conditions was provided. The pilot needs to know the icing severity encountered to prevent exceeding the deicing capability of the aircraft. A cockpit icing severity condition indicator should be installed.

Engine Health Indicator Test

57. The health indicator test (HIT) should be made daily prior to the first flight of the day. The test consists of setting an engine compressor speed (N_G) based on OAT and comparing the indicated torque with a base-line torque. The operator's manual contains base-line temperatures for ambient conditions of -10°C to +50°C. Outside air temperatures less than -10°C were experienced throughout the icing tests. The lack of HIT data in the operator's manual for temperatures less than -10°C precluded the accomplishment of an engine HIT check and is a shortcoming.

ICE DETECTORS

General

58. Two types of ice detector were installed on the test aircraft to compare the icing severity levels experienced by the test aircraft with the LWC established by the CH-47C spray aircraft. A calibrated Rosemount Model 871FA detector (provided by USAAEFA), integral to the prototype deice system, was used to record data. The Rosemount detector was mounted on a pad between the No. 2 engine compartment cooling scoops. A Normalair-Garrett detector (provided by the manufacturer), not integral to the prototype deice system, was also used to record data. The Normalair-Garrett detector was mounted on the right side of the fuselage directly below the maintenance step between the gunner window and the cargo compartment door.

Rosemount Ice Detector

59. The Rosemount Model 871FA icing rate detector provided separate icing rate signals to the Rosemount Model 512P icing rate meter and the on-board instrumentation. The icing rate meter readings were unreliable and constantly

fluctuated from light to moderate and occasionally gave a trace indication while in the icing cloud. By comparison, the rate signal recorded on the on-board instrumentation produced steady indications that compared reasonably well with the icing severities established by the spray aircraft. The inability of the Rosemount Model 512P icing rate meter to produce steady trace, light, or moderate icing rate indication is a shortcoming.

Normalair-Garrett Ice Detector

60. The Normalair-Garret indicator (which measures LWC) was observed to fluctuate from zero to full-scale deflection (2.0 gm/m^3) while in the icing cloud. Usually it indicated LWC between 0.1 and 0.2 gm/m^3, and occasionally the readings correlated with the established LWC, but only for short intervals. Postflight measurements of the ice accreted on the housing that protects the probe were always less than that measured on the FM radio antenna (which is near the probe housing) and the nose of the aircraft. Optimization of the probe location was not possible during the test. Future icing tests of the Normalair-Garrett ice detector should allow for optimization of probe location.

CONCLUSIONS

GENERAL

61. The YUH-60A helicopter does not possess the capability to safely operate in an icing environment without a rotor deice system.

62. Within the scope of this test, the YUH-60A helicopter equipped with a prototype anti-ice/deice system displays potential for operating in a moderate icing environment.

63. The following conclusions were reached upon completion of the YUH-60A helicopter artificial icing test:

a. The electrical power demand of the deice system did not exceed the capability of a single AC generator (para 16).

b. The ice shedding characteristics of the protected portion of the main rotor blades with the deice system operating were satisfactory (para 27).

c. A rotor speed sweep is not a satisfactory means of shedding ice from the inboard section of the blades (para 28).

d. There were no apparent changes in vibration levels attributed to ice accretion on the bifilar weights (para 30).

e. Within the scope of this evaluation, ice protection is not required in the hub area (para 30).

f. Within the scope of this test, ice protection for the pitch change links is not required (para 31).

g. Any change in exhaust gas flow due to the installation of infrared countermeasure devices will require reevaluation of ice accretion characteristics (para 34).

h. Handling qualities appeared qualitatively to be unaltered due to ice accretion on the stabilator (para 34).

i. Autorotational descent performance as a result of ice accumulation was degraded (para 49).

j. There were no significant changes in the main transmission or tail rotor gearbox vibration levels (para 50).

k. Six deficiencies and 14 shortcomings were noted during this test.

DEFICIENCIES AND SHORTCOMINGS

64. The following deficiencies were identified and are listed in order of importance:

a. The inadequate ice protection of the main rotor blades (para 28).

b. The inability to operate the deice system and essential electrical equipment with an AC generator failure (para 17).

c. Excessive loss of engine power available with anti-ice system operation (para 47).

d. Frequency of AFCS failures (para 12).

e. The lack of a system to monitor IPS turbine operation (para 24).

f. The lack of adequate cabin heat at temperatures below -10°C (para 52).

65. The following shortcomings were identified and are listed in order of importance:

a. Presence of accreted ice directly in front of the engine inlet, aft of the pitot-static tube support strut (para 40).

b. Large accumulation of ice on the pilot and copilot windshield frames (para 36).

c. Lack of ice protection on the center windshield (para 37).

d. Inability of the windshield wiper motor to drive the windshield wiper with a large accumulation of ice (para 38).

e. Inability of the windshield wiper drive cable to withstand the torque necessary to drive the windshield wiper with ice accreted (para 23).

f. Inability to jettison the pilot door with ice accreted on the doorframe using the emergency release handle (para 39).

g. Erroneous intermittent illumination of the ICE DETECTED word segment on the caution/advisory panel (para 53).

h. Placement of the deice system failure lights out of the pilot field of view (para 55).

i. Lack of adequate fault isolation will degrade system maintainability (para 18).

j. Absence of a guard to protect the delicate icing probe (para 14).

k. Inability of the Rosemount Model 512P icing rate meter to produce steady trace, light, or moderate icing rate indication (para 58).

l. Ice accreted immediately ahead of the ice detector will adversely influence operation of the ice detector (para 42).

m. Improper manufacture of the pilot windshield (para 22).

n. Lack of HIT data in the operator's manual for temperatures less than -10°C (para 56a).

RECOMMENDATIONS

66. Correct the deficiencies prior to flight in icing conditions.

67. Correct the shortcomings prior to production.

68. The following WARNING should be placed in chapter 10 of the operator's manual (para 29):

WARNING

> Following flight into icing conditions, ice shed from the rotor blades and/or other rotating components presents a hazard to personnel during ground operation and shutdown of the helicopter. Ground personnel should remain well clear of the helicopter during landing, ground operation, and shutdown. Passengers/crewmembers should not exit the helicopter until the rotor has stopped.

69. Further tests should be accomplished with the tail rotor fully immersed in the spray cloud and with infrared countermeasure devices installed (para 33).

70. Proper protection should be provided for all moisture-intolerant components in the engine nacelle (para 41).

71. A cockpit icing severity condition indicator should be installed (para 56).

APPENDIX A. REFERENCES

1. Specification, UTTAS Project Manager, AMC-SS-2222-10000D, "System Specification for Utility Tactical Transport Aircraft System," 10 November 1975.

2. Letter, AVSCOM, DRSAV-EQI, 25 May 1976, subject: Utility Tactical Transport Aircraft System (UTTAS) Artificial Icing Test, AVSCOM Test Directive, Project No. 76-09.

3. Test Plan, USAAEFA, Project No. 74-09, *Artificial Icing Test, Utility Tactical Transport Aircraft System (UTTAS), Sikorsky YUH-60A Helicopter, Boeing YUH-61A Helicopter,* August 1976.

4. Prime Item Development Specification, Sikorsky Aircraft Division of United Technology Corporation, AMC-CP-2222-S1000A, "UTTAS," March 1976.

5. Operator's Manual, Sikorsky Aircraft Division, No. SA4047-25, *Preliminary Operator's Manual, Army Model YUH-60A Helicopter*, 1 December 1975, with Change 2, 15 March 1976 and Icing Supplement, 27 September 1976.

6. Final Report, USAAEFA, Project No. 74-06-1, *Government Competitive Test, Utility Tactical Transport Aircraft System (UTTAS), Sikorsky YUH-60A Helicopter*, to be published.

7. Handbook, All American Engineering Company, SM280B, *Installation, Operation, and Maintenance Instructions, with List of Parts, Helicopter Icing Spray System (HISS)*, 12 November 1973, revised 15 July 1976.

8. Final Report, USAAEFA, Project No. 75-04, *Modified Helicopter Icing Spray System Evaluation*, to be published.

9. Letter, AVSCOM, DRSAV-EQI, 27 September 1976, subject: Safety of Flight Release (SOFR) for YUH-60A Artificial Icing Test.

10. Letter, Sikorsky Aircraft Division, 4 November 1976, subject: Adverse Weather Test Program - Control DAAJ01-73-C-0006(P6A), Modification P00039, as amended by Modification P00043.

11. Technical Report, Environmental Research and Technology, Inc, *Characteristics of a Spray Plume*, April 1976.

12. Instruction Manual, Rosemount Engineering Company, No. 8784, *Ice Detector Model 871FA*, August 1974.

13. Field Manual, FM 1-30, *Meteorology for Army Aviators*, 31 May 1976.

14. Army Regulation, AR 310-25, *Dictionary of United States Army Terms (Short Title: AD)*, 1 March 1969.

APPENDIX B. ANTI-ICE DEICE SYSTEMS DESCRIPTION

ANTI-ICE SYSTEMS

General

1. The anti-ice systems installed on the YUH-60A helicopter use a variety of methods to provide ice protection. Engine bleed air is used to anti-ice the engine inlet and the engine. Additional engine anti-ice protection is provided by hot engine oil and the IPS, which offers limited protection from foreign materials such as ingested ice chunks. Electrical energy is used to anti-ice the pilot and copilot windshields, the pitot tubes, and the struts that support the pitot tubes.

Engine Anti-Icing

2. Engine anti-icing is accomplished by a combination of hot axial compressor discharge air and heat rejection from the air/oil cooler integral to the main engine frame. A hot air anti-icing valve is electrically controlled by the ENG ANTI-ICE switch on the overhead panel. Anti-icing is OFF when electrical power is applied to the solenoid of the combination anti-icing and starting bleed valve assembly. Additionally, the valve will automatically open at an N_G less than 83 percent.

3. Axial compressor discharge air (station 2.5) is bled from the compressor casing at the 7 o'clock position, routed through the anti-icing valve, and delivered to the front frame and swirl frame via ducting (fig. 1). Within the swirl frame, hot air is ducted around the outer casing to each swirl vane. The hot air is circulated within each vane by a series of baffles, then exits from two areas. Approximately 90 percent of this hot air exits at the vane outer trailing edges. The other 10 percent exits through a series of circumferential slots in the swirl frame hub at the aft edge. This arrangement also acts as a "rain step" to preclude water from adhering to the hub and flowing into the compressor. Front frame anti-icing flows through a cored passage in the main frame to the front frame splitter lip, then exits to the main frame scroll and is discharged with IPS air.

4. Anti-icing air is also ducted to the compressor inlet guide vanes (IGV's). A circumferential manifold surrounds the aft flange of the main frame to distribute hot air to the hollow IGV's. Slots in the trailing edge of the IGV's discharge this flow into the compressor inlet. Additionally, hot scavenge oil passing within the scroll vanes in the main frame precludes ice buildup which could result from moisture-laden IPS air.

Engine Inlet Anti-Icing

5. Engine inlet anti-icing is provided by hot axial compressor discharge air which is also electrically controlled by the ENG ANTI-ICE switch on the overhead panel. With the ENG ANTI-ICE switch ON, bleed air passes into inner and outer supply

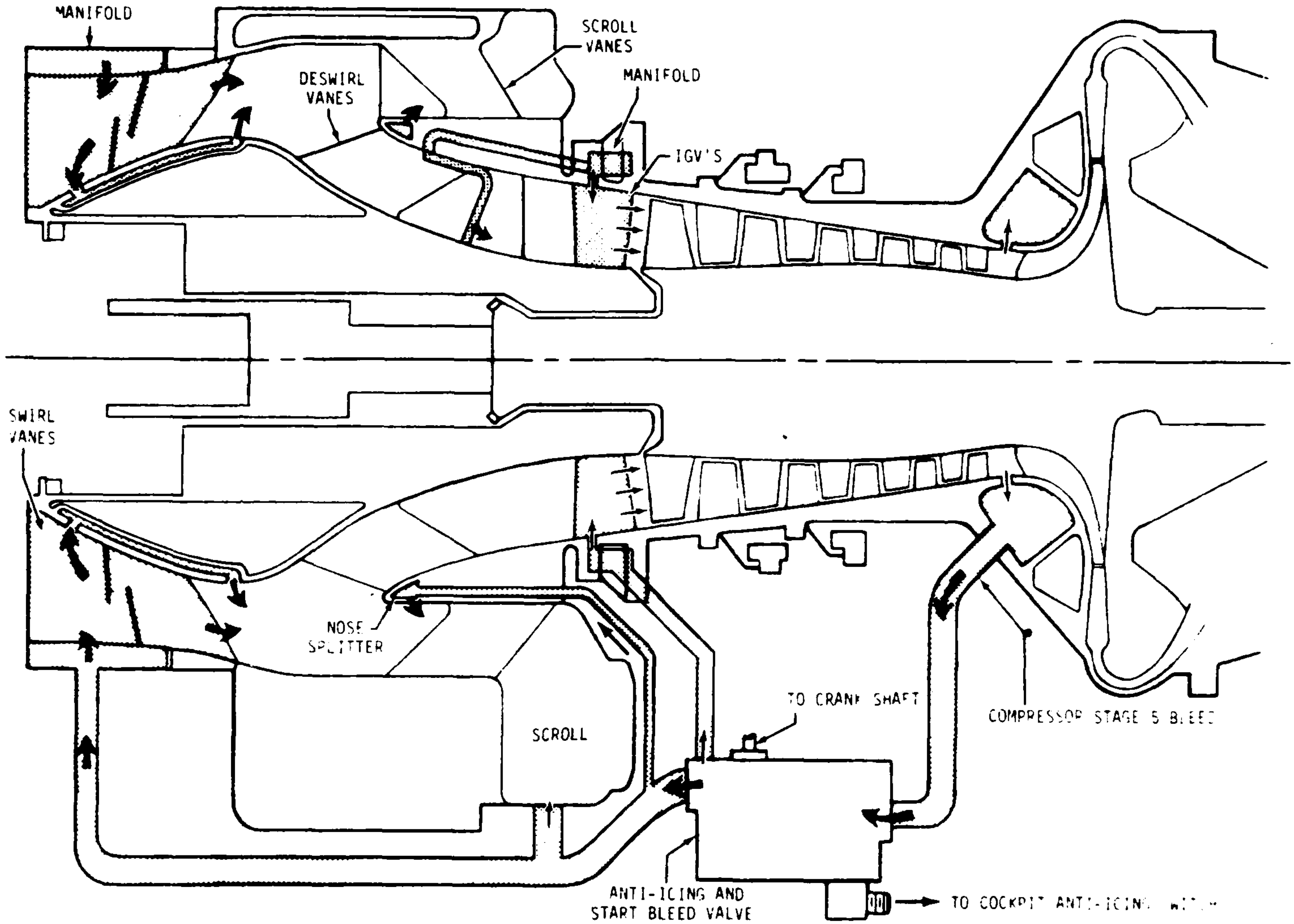

Figure 1. Anti-icing Airflow Schematic.

manifolds which are contained within the inner bullet nose and outer lip of the engine inlet. Anti-icing is then accomplished by a combination of convection and impingement as the bleed air flows between the flexible high-temperature fiberglass wall in the manifolds and the aluminum surface of the inlet. The entire surface of the inlet to the engine swirl frame, to include the bullet nose forebody and the fixed crotch section, is anti-iced in this manner. Exit provisions for the bleed air are provided through slots at the mouth of the inlet on the inboard side, plus an annular slot in the inlet immediately ahead of the swirl frame. A small portion of the slot immediately ahead of the T_2 sensor was blocked so that hot anti-ice exit air would not give a false T_2 signal to the hydromechanical unit (HMU).

Windshield Anti-Ice

6. The pilot and copilot windshields are electrically anti-iced by transparent conductors imbedded between the laminations of the windshields. AC electrical power heats the windshields, while control of the system is through the use of DC electrical power which incorporates circuit breakers for system protection. Two switches located on the upper console (fig. 2), one for the pilot and one for the copilot, turn the windshield anti-ice system on and off. Power to operate the windshield anti-ice system is provided by the No. 1 and No. 2 AC primary buses through circuit breakers marked WSHLD ANTI-ICE PILOT and WSHLD ANTI-ICE COPILOT. Two temperature sensors embedded diagonally across the windshield from each other provide an input to a controller which maintains the windshield surface temperature at approximately 43°C. Additional system protection is provided by a windshield anti-ice system fault-monitoring circuit that prevents windshield burnout. In the event the monitor circuit turns the windshield anti-ice off, the system may be reactivated by cycling the appropriate windshield anti-ice switch. The windshield anti-ice system is fully operational if the auxiliary power unit (APU) generator is the sole source of AC electrical power, except when the backup hydraulic pump is ON, at which time the windshield anti-ice system is automatically disconnected. Figure 3 is a diagram of the windshield anti-ice system.

Pitot-Static Anti-Ice

7. A pitot-static tube heater switch, marked PITOT HEAT ON and OFF, is located on the upper console (fig. 3). When the switch is placed in the ON position, electrical elements in the pitot heads and the supporting struts are turned on and an advisory capsule on the caution/advisory panel, marked PITOT HEAT ON, is illuminated. Electrical power to operate the system is supplied from the No. 1 and No. 2 AC primary buses through circuit breakers marked LEFT PITOT HEAT and RIGHT PITOT HEAT.

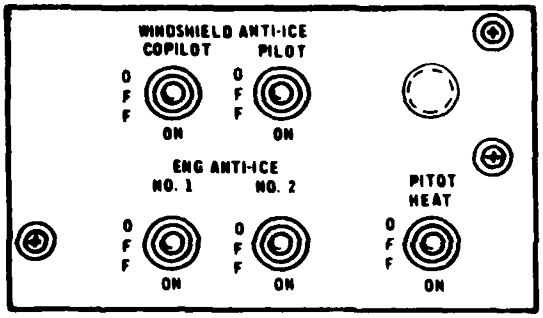

Figure 2. Windshield Anti-ice Panel.

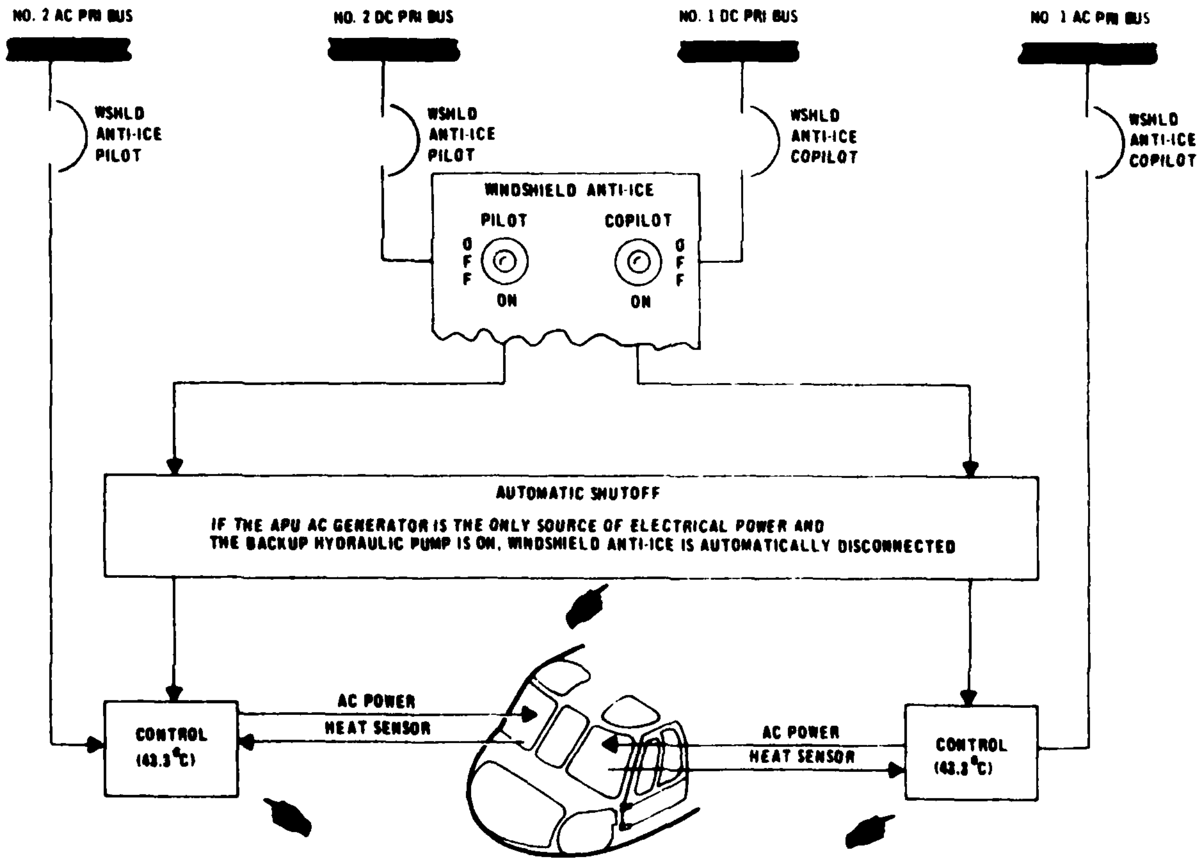

Figure 3. Windshield Anti-ice System Diagram.

DEICE SYSTEM

General

8. The deice system installed in the YUH-60A helicopter was a prototype electrothermal system made up of the following eight subsystems: cockpit control and associated lights; ice detector, two each; outside air temperature (OAT) sensor, three each; controller with two complete sets of logic; distributor; slip ring assemblies, one each for the main and tail rotors; electrothermal heater mats; and deicing engineer control panel. Electrical power from the No. 2 AC generator (115 VAC, 30 kVA, 400 Hz) was used to operate the system, while DC electrical power (28 VDC) from the No. 1 primary DC bus was used to control the system. Total electrical power required for this prototype system was estimated to be 25 kVA. A prerequisite for system operation in any mode was 90 percent rotor speed or greater.

Cockpit Control and Associated Lights

9. The cockpit control panel was located in the left rear corner of the lower console and contained a mode select switch, a test switch, a green system ON light and two amber system malfunction lights. The mode select switch was a three-position switch that turned the system on, illuminated the green press-to-test system ON light when the system was functioning properly, and allowed the pilot to select either the AUTO or MANUAL mode of operation. In the AUTO mode, the system was armed so that once the ice detector detected ice, the deice system commenced operation, with predetermined system OFF times as a function of OAT set on the deicing engineer control panel. When ice was no longer present at the detector, the system automatically shut down and remained armed for the next icing encounter. When the MANUAL mode was selected, the ice detector circuits were bypassed and the system began to function only when commanded at the deicing engineer control panel. System operation was terminated by moving the mode select switch from MANUAL to OFF. The spring-loaded test switch allowed the pilot to make a functional check of the system. The system sequentially applies electrical power for 1 second to each heater zone and system malfunctions, if found, are indicated by amber press-to-test lights on the control panel, one each for the main and tail rotors. If the test switch is held for more than 60 seconds, the test sequence is repeated.

Ice Detectors

10. Two Rosemount Model 871FA ice detectors were provided with the prototype deice system. One detector was attached to the outboard side of each engine cowling between the engine compartment cooling air scoops. The detector installed on the left side of the aircraft was aspirated by engine bleed air and provided the ICE-DETECTED signal used to automatically turn the system on and off when the AUTO mode was selected. The unaspirated detector installed on the right side of the aircraft provided the ICE-DETECTED signal to the Rosemount 512P icing rate meter mounted on the deicing engineer control panel. The icing signal was

then relayed to the caution/advisory panel where it would illuminate the master caution light, the ICE-DETECTED caution capsule, and alert the pilot of an icing encounter.

Outside Air Temperature Sensors

11. Three identical Rosemount 159U OAT sensors were provided with the deice system. All three were mounted on the nose section between the center windshield and the nose door, with a shield installed in front of the sensors to eliminate kinetic heating effects. One sensor was used to provide a temperature signal to the controller that would limit heater mat ON time to 1 second when OAT was 2°C or greater, and the mode select switch was in either the AUTO or MANUAL position. This was the rotor blade overtemperature protection feature of the deice system. This feature provides redundant protection when the mode select switch is left in the AUTO position since ice should not be detected at 2°C and the system should already be shut down. The two remaining sensors provide temperature inputs to the controller to regulate system ON times in the MANUAL or AUTO mode, respectively, since each mode has an independent set of control and logic circuitry.

Controller

12. The controller was located on the deicing engineer control panel in the cargo compartment and contained the control, logic, and failure detection circuits that established system ON and OFF times, provided system protection, and allowed for system test. Although the controller had the capability to establish system ON time based on an input from the OAT sensors, system ON times were manually set at the deicing engineer control panel for a given set of test conditions. System OFF times, which are a function of icing rate, were also manually set at the deicing engineer control panel, since this prototype system only used the ice detector signal to turn the system on and off when the AUTO mode was selected. System protection was provided by the failure detection circuits that sensed a system failure, activated the appropriate malfunction light on the cockpit control panel, and automatically shut the deice system down when a failure occurred in either the controller, the contactor, or the distributor. System protection for the controller was accomplished by establishing high and low system amperage trip points when power was applied to the system. This feature gave protection to the system against overcurrent and undercurrent conditions. The system also shut down when no current was applied. System protection for the contactor was accomplished by monitoring whether the contactor was sticking in the open or closed position, either of which would shut the system down. Failure to return to the start position, failure to step, stepping more than one zone, or system ON times 4 seconds greater than required, are all malfunctions of the distributor that would cause deice system shutdown. System test was accomplished by expediting a deice cycle and letting the failure detection logic check system operation as described above.

13. The contactors (one each for main and tail rotors) were located in the ceiling of the cargo compartment aft of the transmission and provided the interface between system control and system operation. Although the contactors were not physically located with the controller, they are considered components of the controller, since they allow passage of electrical power (115 VAC, 30 kVA, 400 Hz) from the No. 2 AC generator to the heater mats based on inputs from their respective timing circuits.

Distributor

14. The distributor was located on the deicing engineer control panel in the cargo compartment and was a stepping switch that allowed electrical power to be sequentially applied to the heater zone in the main rotor. Electrical power from the main rotor contactor was supplied to the distributor, which divided the system ON time into four equal time segments by sequentially stepping through the four heater zones, based on a time input from the main rotor timing circuit in the controller. Feedback information from the distributor to the controller monitored the distributor's operation and malfunctions detected by the controller caused shutdown of the entire deice system.

Slip Ring Assembly

15. The slip ring assemblies provided a means of transferring electrical power to the main and tail rotor heater mats. For the main rotor, the slip ring was mounted on top of the main rotor head and received its power from the distributor. Power for the tail rotor came from the tail rotor contactor directly to the tail rotor slip ring, which was mounted to the tail rotor gearbox. Both slip ring assemblies were designed with a shear pin to prevent shaft seizure in the event of a bearing seizure.

Electrothermal Heater Mats

16. The electrothermal heater mats were embedded in the leading edge of each main and tail rotor blade. The mats, manufactured by Goodyear Aerospace Corporation, consist of a series of strain-relieved wires running spanwise, woven uniformly (24 wires per inch) into a stabilizing fabric carrier. The main rotor blade mat was divided into four electrically independent heater zones, while each tail rotor blade had only one heater zone. Heater mat coverage for the main rotor blade was 35 to 95 percent spanwise; and 8 percent upper, 12 percent lower chordwise. Heater mat coverage for the tail rotor blades was 48 to 98 percent spanwise, and 16 percent both sides chordwise. Power density for the main and tail rotor blades was 25 and 10 watts per square inch, respectively.

17. The heater mats were applied to the SC 1095 main rotor airfoil (not the GCT main rotor airfoil) by replacing the polyurethane layer with the heater mat. An adhesive, AF-30 manufactured by 3M Company, was then applied to the leading edge from the root end to the tip cap. The AF-30 also provided erosion protection from the inboard portion of the blade (root end to blade station 114,

approximately 36 percent spanwise). A stainless steel leading edge strip provided erosion protection from blade station 114 to blade station 208 (approximately 65 percent spanwise), and the remainder of the leading edge erosion protection, out to the tip cap, was provided by the production leading edge nickel abrasion strip.

18. The heater mats were applied to the tail rotor blade essentially as described above, the only difference being in the dimension of the erosion shield and the AF-30 coverage.

Deicing Engineer Control Panel

19. The deicing engineer control panel was located in the aft section of the cargo compartment facing aft and provided a means of monitoring and adjusting the deice system while in flight (photo 1). Eight temperature transducers embedded in one main rotor blade and two temperature transducers embedded in one tail rotor blade provided a means of measuring blade surface temperature during system operation. The temperatures were then displayed by means of 10 visual indicators mounted on the deicing engineer control panel. Additional indicators of system operation included lights that illuminated when electrical power was being applied to either the main or tail rotor heater mats and a Rosemount 512P icing rate indicator. One switch installed on the control panel simulated ice detected and provided the controller with a false ICE-DETECTED signal. Another switch provided an ice detector test feature and also turned the Rosemount detector on and off. The system was adjusted through two banks of control potentiometers, also located on the control panel, that allowed for independently setting main and tail rotor system ON and OFF times. Since the controller had two identical sets of circuitry, one bank was for the AUTO mode and the other for the MANUAL mode. By monitoring the blade surface temperature, the deice engineer could select any desired setting, as follows:

Main rotor zone heating time	1 to 24 seconds
Tail rotor zone heating time	1 to 40 seconds
Main rotor OFF time	1 to 4 minutes
Tail rotor OFF time	0.3 to 2 minutes

20. In addition to the contractor-provided deice system, an indicator and a three-position ON/OFF/TEST switch for the Normalair-Garrett ice detector were installed on the deicing engineer control panel.

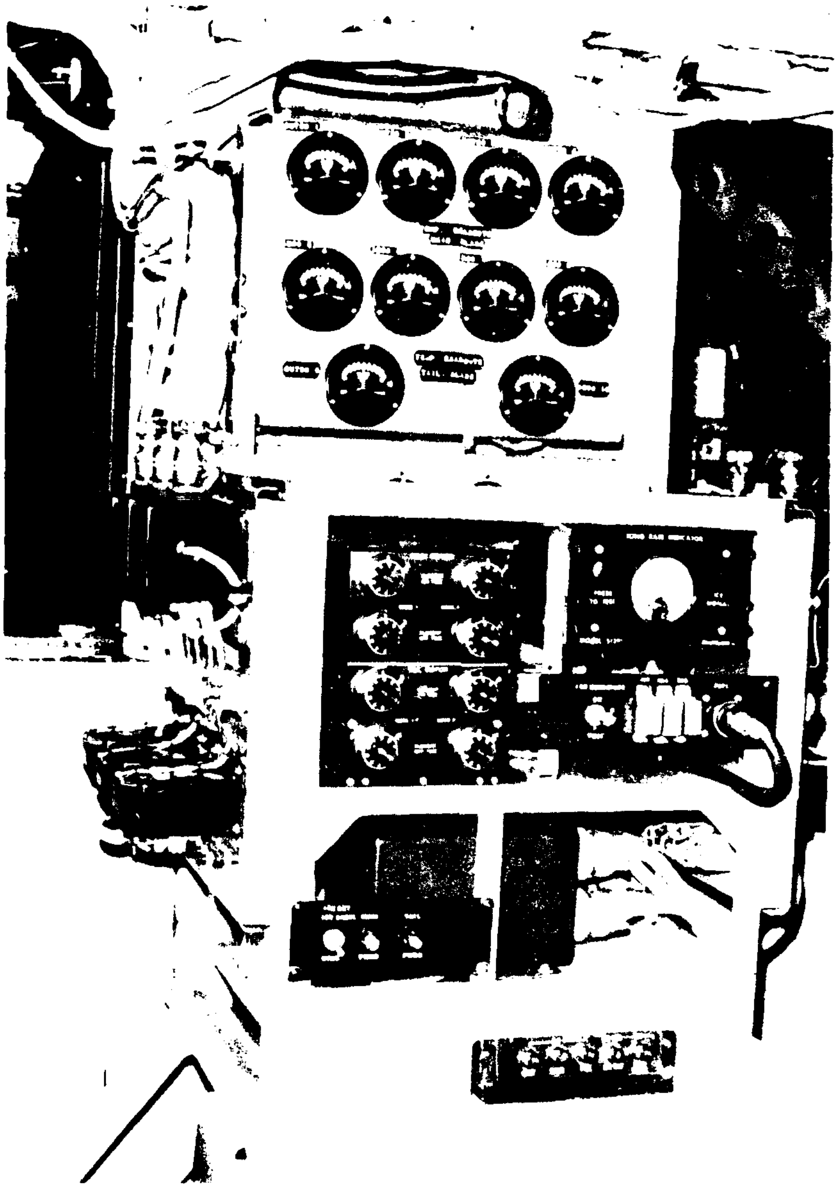

Photo 1. Deicing Engineer Control Panel.

APPENDIX C. HELICOPTER ICING SPRAY SYSTEM DESCRIPTION

1. The HISS is carried on board a CH-47C aircraft. The icing spray system equipment consists of a spray boom, boom supports, boom hydraulic actuators, an 1800-gallon unpressurized water tank, and operator control equipment (fig. 1). The spray boom consists of two 27-foot center sections and two 16.5-foot outer sections. The total weight of the system is approximately 4700 pounds empty. With the boom fully extended, the upper center section is located in a horizontal plane 15 feet below the aircraft and the lower center section 20 feet below. The booms are fully jettisonable in both the fully extended and stowed positions. The water is also jettisonable (total load of 1800 gallons) in approximately 10 seconds with the boom in any position. A total of 174 nozzle locations are provided on the spray boom. Nozzles are installed at 54 of these locations. A bleed air supply from the aircraft engines is used to atomize the water at the nozzles. For a more detailed description of the icing spray system, see reference 7, appendix A.

2. The LWC and water droplet size distribution of the spray cloud are controlled by varying the water flow rate and the distance of the test aircraft behind the spray aircraft. Controls and indicators for the water flow rate and bleed air pressure are located on the water supply tank. A radar altimeter is mounted in the rear cargo door opening of the CH-47C and is directed aft. The distance between the test and spray aircraft is measured by the radar altimeter and the information is presented in the spray aircraft cockpit. The methods used to establish the desired LWC are presented in appendix E. A detailed description of the spray cloud characteristics is contained in reference 11, appendix A.

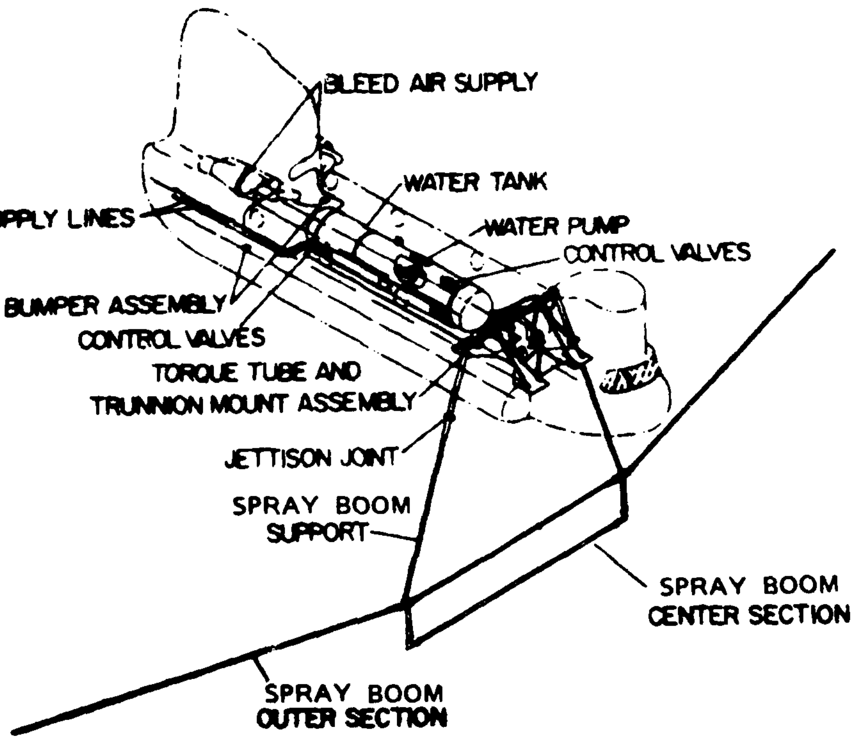

Figure 1. Helicopter Icing Spray System Schematic.

APPENDIX D. INSTRUMENTATION AND SPECIAL EQUIPMENT

INSTRUMENTATION

1. In addition to, or instead of, standard aircraft instruments, sensitive calibrated instrumentation was installed aboard the test aircraft and maintained by the contractor. Data were recorded from the cockpit instrumentation and the specially installed instrumentation system. Data were recorded on flight data cards and magnetic tape (PCM and FM). Selected parameters were observed real time via air-to-ground telemetry (TM).

2. The sensitive instrumentation, calibrated ship's system instrumentation, and related special equipment installed are listed below.

Pilot/Copilot Panel

Airspeed (ship's system)
Altitude (ship's system)
Rate of climb/descent (ship's system)
Free air temperature (ship's system)
Rotor speed (digital)
Engine torque (both engines)
Engine turbine inlet temperature (both engines)
Engine gas generator speed (both engines)
Engine power turbine speed (both engines)
Engine inlet particle separator differential
    pressure (both engines)
Stabilator position
Control position:
    Longitudinal
    Lateral
    Directional
    Collective
Star load

Pilot/Copilot Station

Event switch
Visual ice accretion probe
Deice controls and lights
Vibration meter (Chadwick-Helimuth)

USAAEFA Engineer Station

Instrumentation controls and lights
Main and tail rotor camera switches
Event switch
Time of day
Run number
Fuel remaining
Free air temperature

Deicing Engineer Station

Icing rate (Rosemount 871FA)
Icing condition (Normalair-Garrett)
Main rotor blade surface temperatures (8)
Tail rotor blade surface temperatures (2)
Main rotor deice system potentiometers (4)
Tail rotor deice system potentiometers (4)
Rosemount ice detector test switch

Digital (PCM) Data Parameters

Airspeed (ship's system)
Altitude (ship's system)
Rate of climb (ship's system)
Free air temperature
Rotor speed
Engine gas generator speed (both engines)
Engine power turbine speed (both engines)
Engine output shaft torque (both engines)
Engine turbine gas temperature (both engines)
Fuel flow (both engines)
Fuel used (both engines)
Engine inlet particle separator duct
    differential pressure (both engines)
Control position:
    Longitudinal
    Lateral
    Directional
    Collective
    Engine condition lever (both engines)
Aircraft pitch attitude
Tail rotor shaft torque
Stabilator position
Main rotor camera correlation pulse

Tail rotor camera correlation pulse
Main rotor blade surface temperatures (8)
Tail rotor blade surface temperatures (2)
Engine anti-ice valve position (No. 1)
Engine inlet duct anti-ice valve position (No. 1)
Generator (No. 1):
- Frequency
- Voltage (A phase)
- Current (A, B, and C phases)

Deice/anti-ice system electrical parameters:
- Main rotor voltage (A, B, and C phases)
- Main rotor current (A, B, and C phases)
- Tail rotor voltage (A, B, and C phases)
- Tail rotor current (A, B, and C phases)
- Windshield voltage (A, B, and C phases)

Rosemount icing rate
Normalair-Garrett icing condition
Time of day
Run number
Pilot and engineer event pulse

<u>Analog (FM) Data Parameters</u>

Vibration (accelerometer location):
- Pilot station vertical
- Pilot station lateral
- Pilot station longitudinal
- Aircraft cg vertical
- Aircraft cg lateral
- Aircraft cg longitudinal
- Main transmission (top) vertical
- Main transmission (top) lateral
- Main transmission (top) longitudinal
- Tail rotor gearbox vertical
- Tail rotor gearbox lateral
- Tail rotor gearbox longitudinal

3. In addition to standard aircraft instruments, sensitive calibrated instrumentation was installed aboard the CH-47C spray aircraft. This instrumentation was used to establish the desired test conditions during the icing flights and is listed below.

Airspeed
Altitude
Free air temperature
Dew point
Water flow rate
Bleed air pressure

Radar distance (separation between test
and spray aircraft)

SPECIAL EQUIPMENT

Camera Systems

4. Two Teledyne 16mm camera systems, Model DBM 44, were installed on the test aircraft to photograph the main and tail rotor blades in flight. The camera film magazine held 200 feet of film and camera shutter speeds of up to 400 frames per second (fps) were available. Another 16mm high-speed hand-held motion picture camera was located on board the chase aircraft and was used to document the test aircraft both in the spray cloud and after exit from the cloud. Additionally, 35mm color slide and black and white still cameras were used for documentation both in the air and on the ground following each icing flight.

5. The main rotor camera was mounted on top of the main rotor hub assembly (photo 1). It was positioned over one of the four main blades so that the top of the blade was visible out to approximately 80 percent of its span. The camera was encased in a specially built box with an electrically heated window in front of the camera lens. A shutter speed of 250 fps was used.

6. The tail rotor camera was mounted on the right side of the tail cone facing aft toward the tail rotor (photo 2). The camera installation was covered with an electrically heated fairing to prevent ice buildup. A shutter speed of 400 fps was used.

Ice Detectors

7. Two ice detectors (a Rosemount Model 871FA and a Normalair-Garrett) were installed on the test aircraft to correlate the icing severity levels experienced by the test aircraft with the LWC established by the CH-47C spray aircraft. A third ice detector (Rosemount Model 871FA) was installed as part of the aircraft deice system (para 10, app B). Additionally, a visual ice accretion probe was installed on the test aircraft to document ice accumulation.

Rosemount Model 871FA Ice Detector:

8. The Rosemount Model 871FA ice detector is an electromechanical device which transmits an electronic signal when a specified thickness of ice is present on the sensing probe. Two Model 871FA detectors were mounted on the test aircraft. The contractor ice detector was aspirated and used to trigger the aircraft deice system ON and OFF in the AUTO mode. This deice system detector was mounted on a pad located between the left engine compartment cooling scoops (photo 3). The instrumentation detector was mounted on a pad located between the right engine compartment cooling scoops (photo 4). The instrumentation detector incorporated a Rosemount Model 512P icing rate meter and test switch

Photo 1. 16mm Motion Picture Camera Installation on Main Rotor Hub Assembly.

Photo 2. 16mm Motion Picture Tail Rotor Camera Installation.

Photo 3. Aspirated Rosemount Model 871A Ice Detector Probe **Installation.**

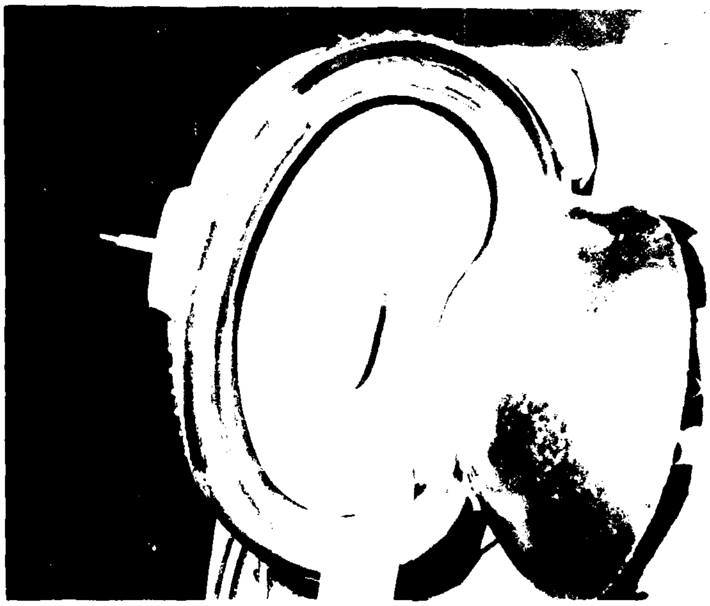

Photo 4. Rosemount Model 871FA Ice Detector Probe Installation.

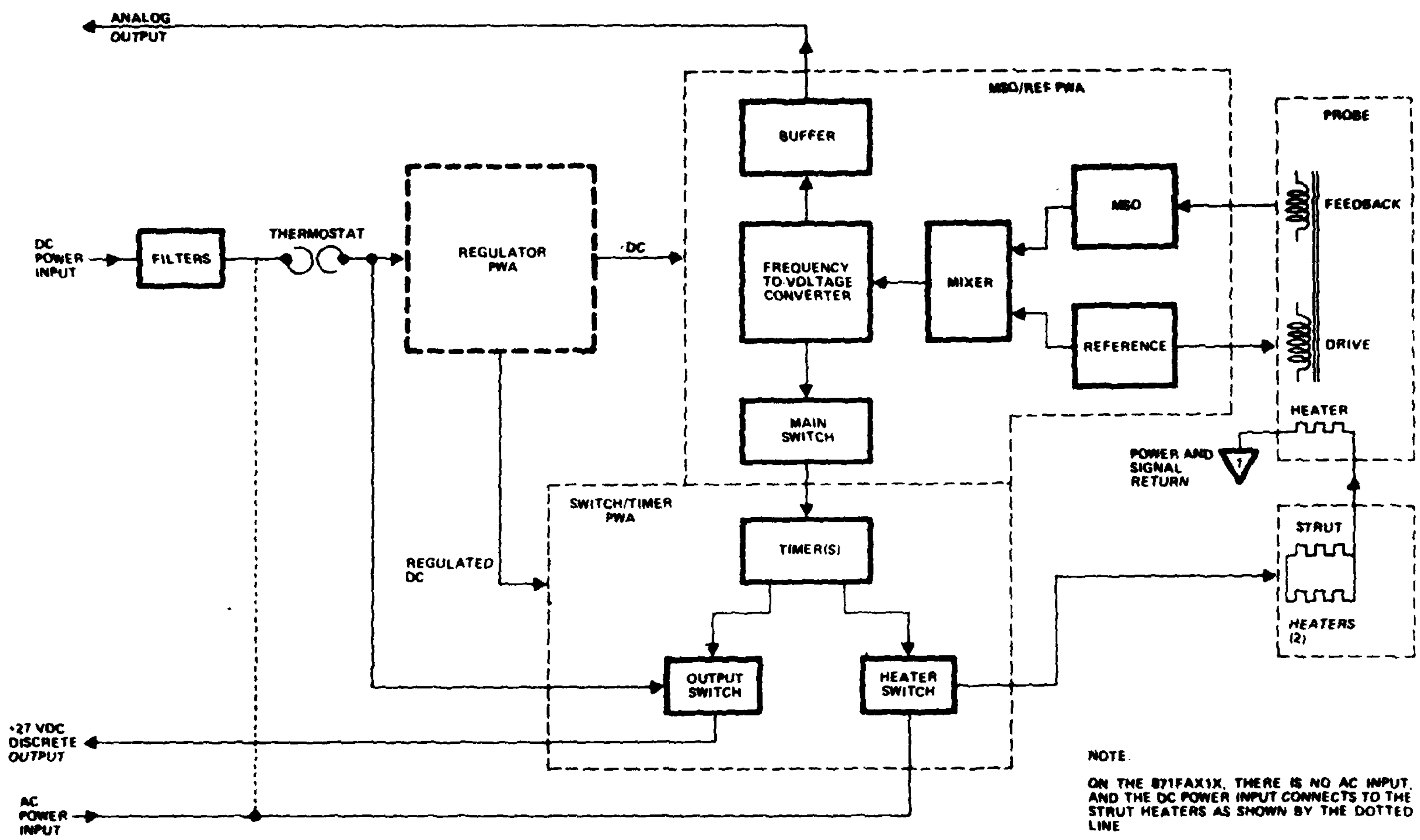

Figure 1. Rosemount Model 871A Schematic.

installed in the aft cargo compartment on the deice engineer panel (photo 5). A block diagram of the detector operation is shown in figure 1.

9. The operation of the two detectors is identical. The sensing element of the ice detector is an axially vibrating tube whose natural frequency changes with ice accumulation. Tube vibration is achieved with a magnetostrictive oscillator (MSO). The reference oscillator signal is summed with the signal from the MSO to produce a difference frequency (the output of the mixer). The frequency-to-voltage converter changes the frequency difference to a voltage, and when this voltage reaches a preset value corresponding to the accumulation of 0.020 inch (0.5mm) of ice, an output signal is provided to the timer. The timer initiates the probe heating cycle, which purges the probe of the accumulated ice. Also, a constant voltage output signal is provided. The signal from the instrumentation detector was recorded on the data package magnetic tape. After the probe heating cycle is completed the probe is ready to accrete ice and the sequence is repeated (ref 12, app A).

10. The frequency-to-voltage converter of the MSO also provides a variable voltage analog output corresponding to ice thickness. The instrumentation detector signal was differentiated and was displayed on the Rosemount Model 512P icing rate meter on the deice engineer panel.

11. The press-to-test button on the deice engineer panel was provided to check system operation. Depressing and holding the button creates a difference frequency which simulated ice accumulation on the probe. Proper system operation was indicated by illumination of a red light and deflection of the icing severity needle.

Normalair-Garrett Ice Detector:

12. The Normalair-Garrett ice detector is an inferential type detector. Unlike the Rosemount detector, which allows ice to accrete on a probe, the Garrett detector senses the amount of free water in the atmosphere. Specifically, the system measures the impingement and rate of supercooled liquid water and icing surface temperature. The system consists of three major components: moisture-sensing head, control module, and icing severity indicator.

13. The Normalair-Garrett moisture-sensing head was mounted on the test aircraft fuselage just aft of the right gunner window and below the maintenance step (photo 6). The water and skin temperature-sensing head consists of two cylindrical heater/sensor probes mounted on a short airfoil section mast. The front heater is exposed directly to the airflow and impinging water droplets. A cross-section view of the moisture-sensing head is shown in figure 2. The rear heater is housed within the inertia separator, which prevents any water droplets impinging on its surface. Both heaters are maintained at a constant electrical temperature by the electronic control module. The physical proportions of the two probes and the recovery factor of the inertia separator give equal cooling to the two probes under dry air conditions. Therefore, the same electrical power is required to make the temperature of the two probes equal. When supercooled water droplets are present,

Photo 5. Rosemount Model 512[illegible] Icing Rate Indicator.

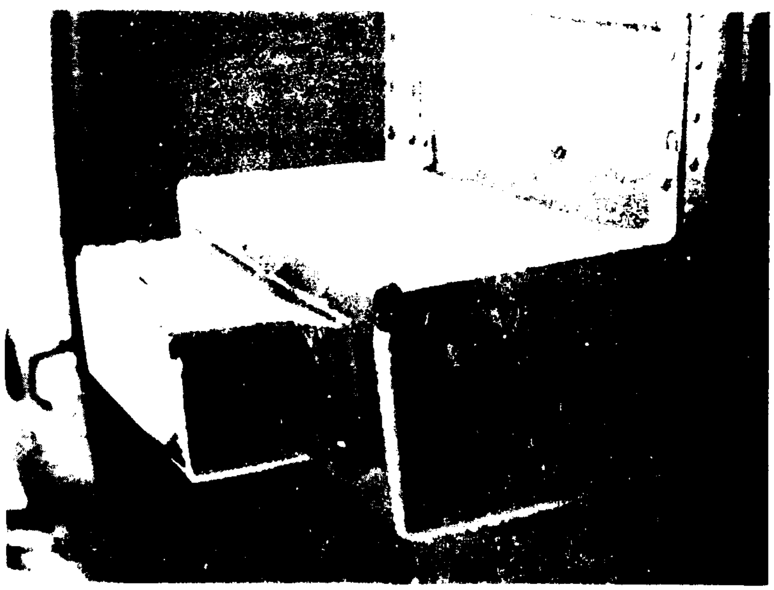

Photo 6. Normalair Garrett Ice Detector Probe Installation.

an increase in power is required by the front probe to maintain equality of temperature with the rear probe. The difference in power levels between the front and rear probes is therefore a function of the water evaporated from the front probe in unit time. This power difference is processed by the electronic control module and presented on the cockpit indicator (photo 7) in terms of icing severity (gm/m^3).

14. The icing surface temperature is obtained indirectly by a temperature sensor, which is part of the servo control system, maintaining the sensing head support mast at a temperature set above 0°C. This temperature signal is used to inhibit the indicator at that skin temperature at which no ice can form.

15. In order to check the complete system for correct functioning, a self-test facility is provided on the cockpit panel. When the self-test switch is activated, an electrical imbalance of the front probe temperature is created, which simulates cooling of the probe by water droplets. At the same time, the temperature sensor cut-out is disconnected to allow the check to be carried out above freezing conditions. The resulting icing severity indicator deflection and warning lamp illumination indicate that both the sensing head and control circuits are operational.

Visual Ice Accretion Probe

16. A visual ice accretion indicator probe was fabricated and installed on the test aircraft. It was used to give additional visual cues of ice buildup on the aircraft fuselage. The probe was composed of a small symmetrical airfoil section (OH-6A tail rotor blade sections) with 3/16-inch diameter steel rod protruding outward from the leading edge at the center span. The protruding rod was painted with 1/4-inch stripes of contrasting colors which provided a comparison basis for visual ice measurements. The probe was mounted on the left cockpit door just below the window. Photo 8 shows the installation of the visual ice accretion probe.

Telemetry and Data Reduction System

17. A portable TM monitoring and data reduction system was fabricated to allow on-site data analysis. It consisted of the following:

Nems-Clarke Type R10376 solid state TM receiver
EMR-Schlumberger Model 720 PCM bit synchronizer
EMR-Schlumberger Model 2731 PCM frame synchronizer
EMR-Schlumberger Model 713 programmable word selector
Hewlett-Packard Model 5245L electronic counter
Hewlett-Packard Model 4204A oscillator

18. The TM receiver had a line-of-sight range of approximately 20 to 30 nautical miles and monitored signals on a 1435- to 1540-MHz band. The system converted these signals into a real time display of 12 PCM data channels on the brush recorders and 6 FM data channels on the oscillograph. The channels monitored during a flight were chosen by the project engineer from among any of the channels

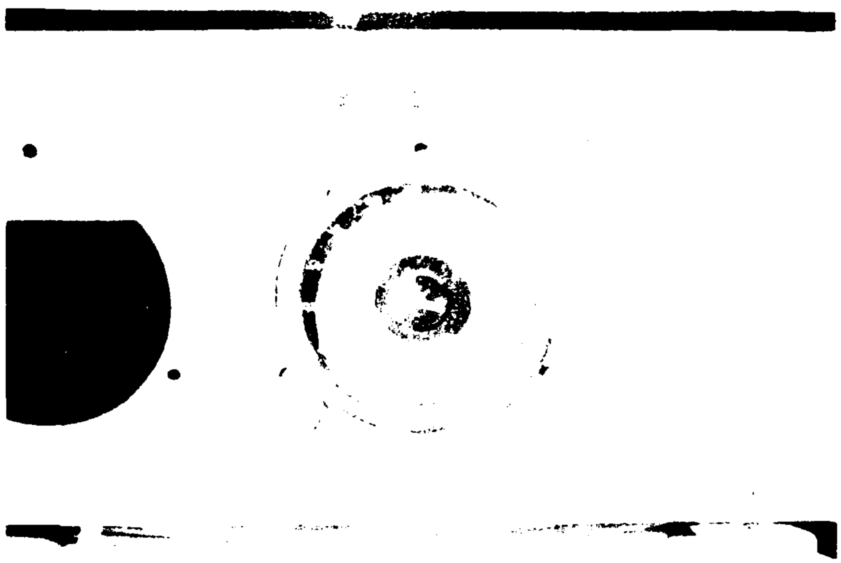

Photo [illegible] ...ication.

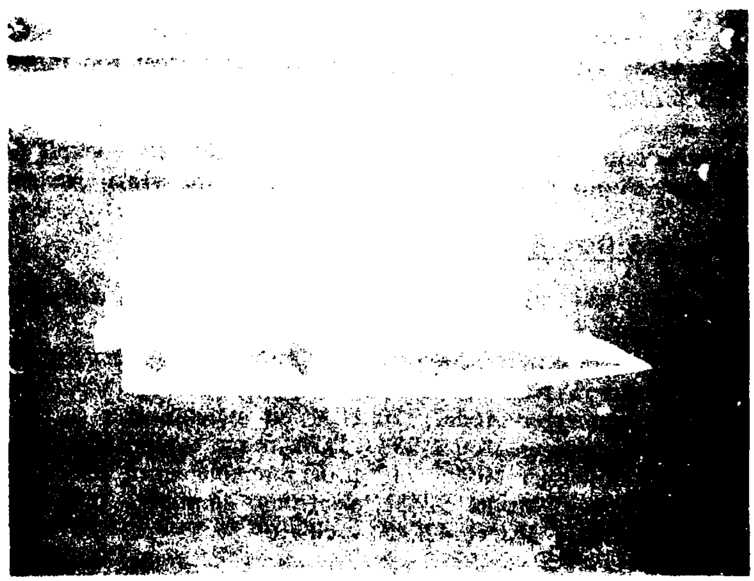

Photo 8. Visual Ice Accretion Indicator Probe Installation on Copilot's Door.

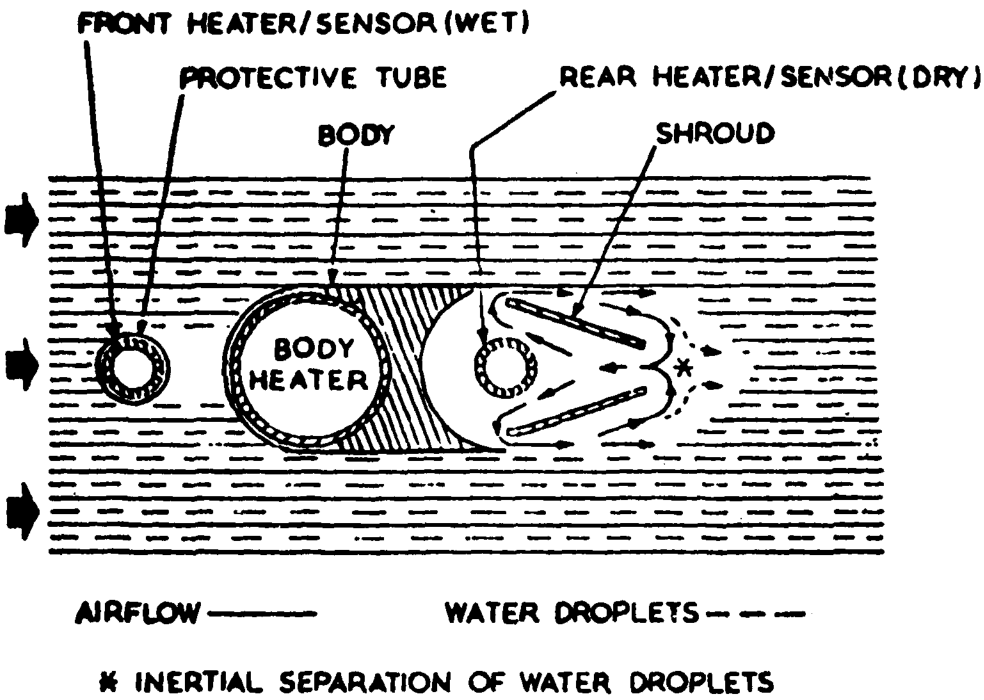

Figure 2. Cross-sectional View of the Normalair-Garrett Probe.

being recorded by the airborne magnetic tape system. The channels displayed could be changed at any time during the flight.

19. The package allowed for postflight strip-out of the flight tape. Each time the flight tape was run through the system, 12 PCM and 6 FM channels could be processed. The electronic counter allowed actual PCM data counts to be compared with pen movements. The flight tape could be rerun until all desired data channels were stripped out. The system allowed for a tape search for a specified time slice and a digital display of the data.

APPENDIX E. TEST TECHNIQUES AND DATA ANALYSIS METHODS

TEST TECHNIQUES

General

1. The deice system tested on the YUH-60A was a prototype system. Therefore, a build-up program was used to gain experience with flight in icing conditions. Three types of flights were used to establish one test point of the test matrix: accretion-only flights, deice system check flights, and long immersion flights (fig. 1). The procedure remained the same for each flight up to entry into the spray cloud. All anti-ice systems (*ie*, pitot heat, windshield anti-ice, engine, and engine air induction system anti-ice) were activated while enroute to the test area. After reaching the test altitude, base-line autorotation and level flight performance data were obtained. Once ready to enter the spray cloud, the test aircraft did so from a position below and approximately 200 feet behind the spray aircraft. Test and spray aircraft separation distance was maintained during the icing flight by information relayed from the spray aircraft. The magnetic tape recording system was activated just prior to entering the cloud and remained on until exiting from it. Test airspeed and outside air temperature while in the cloud were established with the calibrated airspeed system of the spray aircraft. All flights were flown with a predetermined LWC and outside air temperature.

2. The accretion-only flights were conducted to establish OFF times for the deice system. For these flights, the test aircraft entered the spray cloud for a specific time interval or until 1/8 inch of ice accumulated on the visual probe, whichever occurred first. The procedure was then to exit the spray cloud, obtain a stabilized level flight trim record, and return to the landing area as soon as practical.

3. Once the OFF time was determined for a particular LWC, flights were conducted to test the deice system operation and optimize deice system ON and OFF times. The deice system was activated for one deice cycle just before entry into the spray cloud, then the test aircraft entered and remained in the spray cloud until two deice cycles were complete. The test aircraft exited the cloud and a level flight trim record was obtained. If necessary, adjustments to the deice system were made in flight and the cloud was reentered. When the the deice system was judged to be optimized for the test-day conditions the test aircraft returned to the landing area.

4. The final flight for each test point was conducted with the optimized deice system. Entry procedures into the spray cloud were the same as the deice system check flights. The amount of water the spray aircraft had on board and the necessary flow rate combined to establish the maximum time the spray cloud was available. Flight continued in the spray cloud until a test aircraft limitation (*ie*,

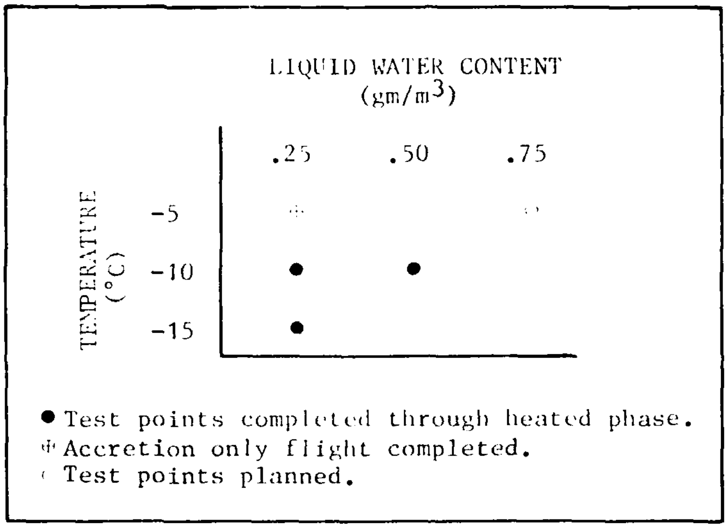

Figure 1. Test Matrix Liquid Water Content.

power, system failure, etc) was reached or the deice cycle nearest the time limit of the HISS. Vibration and performance parameters were monitored continuously during each flight. After the test aircraft exited the cloud, level flight and autorotation data were recorded and the aircraft then returned to the landing area.

5. A progressive build-up procedure was used during the flight testing. The approach was to start at the lowest LWC and warmest temperature and incrementally increase LWC and decrease temperature. As confidence was gained in the deice system and the aircraft's ability to cope with the icing environment, the requirement for flights of increasing length was eliminated and long immersion flights in the icing environment were conducted following verification of system ON and OFF times for a given test condition.

Ice Accretion

6. Ice accretion was determined in flight using the visual ice accretion probe indicator. The visual probe was monitored by the copilot during flight in the spray cloud. The deice engineer used a Rosemount icing rate meter to measure ice accretion rates and a Normalair-Garrett icing condition indicator to monitor LWC.

7. Ice accretion was documented using two high-speed motion picture cameras mounted on the test aircraft and hand-held, high-speed motion picture cameras photographing from both the chase aircraft and the spray aircraft. Postflight photographs were made to document the ice remaining on the individual components of the airframe and rotors.

Level Flight Performance

8. Level flight performance data were obtained by establishing trim level flight at the test airspeed, altitude, and outside air temperature, using the test aircraft calibrated instruments. Data were recorded before icing the test helicopter and again after icing was completed. The same trim true airspeed was used throughout the flight testing.

9. Engine and engine inlet anti-ice system performance data were obtained in conjunction with the icing flights. The test aircraft was stabilized in trimmed level flight at the various test altitudes and temperatures. Testing was conducted with all anti-ice systems OFF for base-line data, with engine anti-ice ON only, and with all anti-ice systems ON. The cabin heater was turned on and the temperature controller was set to maximum on all test flights.

Autorotational Descent Performance

10. Autorotational descent performance data were obtained on those flights designated as long immersion flights and were evaluated at the recommended airspeed for minimum rate of descent. Base-line autorotational descent data were recorded near the test altitude with no ice accumulation on the test aircraft. After icing the aircraft autorotational descent data were again recorded. Changes in

vertical rates of descent, collective control position, and stabilized aurotorational rotor speed were noted.

Weight and Balance

11. The weight and balance of the test aircraft were determined by weighing the aircraft after all airframe modifications and instrumentation changes were completed.

HISS Flow Rate Calculation Method

12. Water flow rate of the HISS, to establish the desired icing severity level for each test flight, was determined using the following technique. The CH-47C spray aircraft used installed calibrated instruments to establish airspeed, altitude, and static air temperature for the desired test condition. The frost point was obtained by utilizing a Cambridge thermoelectric dew-point hygrometer. The frost point was then converted to a dew point using table 1, which was furnished by the instrument manufacturer.

Saturation vapor pressure (millibars) for the dew point and static air temperature was obtained from table 2.

Relative humidity was then computed using the values obtained from table 2 and equation 1:

$$Rh = \frac{P_{VS}}{P_W} \times 100 \qquad (1)$$

Where:

Rh = Relative humidity (percent)

P_{VS} = Saturation vapor pressure for dew point (millibars)

P_W = Saturation vapor pressure for static air temperature (millibars)

13. The decay LWC, which is the spray cloud evaporation rate, was then computed using equation 2.

$$LWC_D = \frac{G(100 - Rh)}{4.5G_0} \qquad (2)$$

Table 1. Cambridge Thermoelectric Dew Point Hygrometer Conversion Values (Degrees Centigrade).

Frost Point	Dew Point	Frost Point	Dew Point	Frost Point	Dew Point	Frost Point	Dew Point
-0.0	-0.1	-6.5	-7.3	-13.0	-14.5	-19.5	-21.1
-0.5	-0.7	-7.0	-7.9	-13.5	-15.0	-20.0	-22.2
-1.0	-1.2	-7.5	-8.4	-14.0	-15.6	-20.5	-22.8
-1.5	-1.8	-8.0	-9.0	-14.5	-16.2	-21.0	-23.3
-2.0	-2.3	-8.5	-9.5	-15.0	-16.7	-21.5	-23.9
-2.5	-2.9	-9.0	-10.1	-15.5	-17.3	-22.0	-24.5
-3.0	-3.4	-9.5	-10.6	-16.0	-17.8	-22.5	-25.0
-3.5	-4.0	-10.0	-11.2	-16.5	-18.4	-23.0	-25.6
-4.0	-4.5	-10.5	-11.7	-17.0	-18.9	-23.5	-26.1
-4.5	-5.1	-11.0	-12.3	-17.5	-19.5	-24.0	-26.7
-5.0	-5.6	-11.5	-12.8	-18.0	-20.0	-24.5	-27.2
-5.5	-6.2	-12.0	-13.4	-18.5	-20.6	-25.0	-27.8
-6.0	-6.7	-12.5	-13.9	-19.0	-21.1	-25.5	-28.3

Temperature °C	.0	.1	.2	.3	.4	.5	.6	.7	.8	.9
-25	0.8070	0.7997	0.7926	0.7854	0.7783	0.7713	0.7643	0.7574	0.7506	0.7438
-24	0.8827	0.8748	0.8671	0.859[illegible]	0.8517	0.8441	0.8366	0.8291	0.8217	0.8143
-23	0.9649	0.9564	0.9479	0.9396	0.9313	0.9230	0.9148	0.9067	0.8986	0.8906
-22	1.0538	1.0446	1.0354	1.0264	1.0173	1.0084	0.9995	0.9908	0.9821	0.9734
-21	1.1500	1.1400	1.1301	1.1203	1.1106	1.1009	1.0913	1.0818	1.0724	1.0631
-20	1.2540	1.2432	1.2325	1.2219	1.2114	1.2010	1.1906	1.1804	1.1702	1.1600
-19	1.3664	1.3548	1.3548	1.3318	1.3204	1.3091	1.2979	1.2868	1.2758	1.2648
-18	1.4877	1.4751	1.4627	1.4503	1.4381	1.4259	1.4138	1.4018	1.3899	1.3781
-17	1.6186	1.6051	1.5916	1.5783	1.5650	1.5519	1.5389	1.5259	1.5131	1.5003
-16	1.7597	1.7451	1.7306	1.7163	1.7020	1.6879	1.6738	1.6599	1.6460	1.6323
-15	1.9118	1.8961	1.8805	1.8650	1.8496	1.8343	1.8191	1.8041	1.7892	1.7744
-14	2.0755	2.0586	2.0418	2.0251	2.0085	1.9921	1.9758	1.9596	1.9435	1.9276
-13	2.2515	2.2333	2.2153	2.1973	2.1795	2.1619	2.1444	2.1270	2.1097	2.0925
-12	2.4409	2.4213	2.4019	2.3826	2.3635	2.3445	2.3256	2.3069	2.2883	2.2698
-11	2.6443	2.6233	2.6024	2.5817	2.5612	2.5408	2.5205	2.5004	2.4804	2.4606
-10	2.8627	2.8402	2.8178	2.7956	2.7735	2.7516	2.7298	2.7082	2.6868	2.6655
- 9	3.0971	3.0729	3.0489	3.0250	3.0013	2.9778	2.9544	2.9313	2.9082	2.8854
- 8	3.3484	3.3225	3.2967	3.2711	3.2457	3.2205	3.1955	3.1706	3.1459	3.1214
- 7	3.6177	3.5899	3.5623	3.5349	3.5077	3.4807	3.4539	3.4272	3.4008	3.3745
- 6	3.9061	3.8764	3.8468	3.8175	3.7883	3.7594	3.7307	3.7021	3.6738	3.6456
- 5	4.2148	4.1830	4.1514	4.1200	4.0888	4.0579	4.0271	3.9966	3.9662	3.9361
- 4	4.5451	4.5111	4.4773	4.4437	4.4103	4.3772	4.3443	4.3116	4.2791	4.2468
- 3	4.8981	4.8617	4.8256	4.7897	4.7541	4.7187	4.6835	4.6486	4.6138	4.5794
- 2	5.2753	5.2364	5.1979	5.1595	5.1214	5.0836	5.0460	5.0087	4.9716	4.9347
- 1	5.6780	5.6365	5.5953	5.5544	5.5138	5.4734	5.4333	5.3934	5.3538	5.3144
- 0	6.1078	6.0636	6.0196	5.9759	5.9325	5.8894	5.8466	5.8040	5.7617	5.7197

Table 2. Saturation Vapor Pressure Over Water.
(Millibars)

Where:

LWC_D = Decay liquid water content (percent/second)

G = Thermodynamic function (centimeter^2/second)

Rh = Relative humidity (percent) (obtained from equation 1)

G_o = 60 x 10^{-8} centimeter^2/second (constant)

The value for the thermodynamic function G used in equation 2 was obtained from figure 2 using the static air temperature indicated by the HISS aircraft. Pressure dependence of G is small, so that values for 1000 millibars given in figure 2 were satisfactory for the test altitudes.

The programmed LWC based on the desired test condition was then corrected for evaporation using the decay LWC calculated above and equation 3.

$$LWC_C = \left(\frac{LWC_D}{100}\right)\left(\frac{D}{1.6889V_T}\right)(LWC_P) + LWC_P \tag{3}$$

Where:

LWC_C = *Corrected liquid water content* (gm/m^3)

LWC_D = Decay liquid water content (percent/second)

D = 200 feet (constant distance between test and spray aircraft maintained during this test)

1.6889 = Conversion factor (ft/sec/kt)

V_t = 90 knots (constant test airspeed)

LWC_P = Programmed liquid water content (gm/m^3)

14. The corrected LWC and figure 3 were then used to determine the required water flow rate. The flow rate obtained from figure 3 and a constant bleed air pressure of 15 pounds per square inch (gauge) were used to establish the spray cloud.

DATA ANALYSIS METHODS

15. The icing severity was a function of time in the spray cloud, temperature, and LWC. The programmed icing severity was compared with the Rosemount and Garrett ice detectors. Ice accretion was measured in flight using the visual probe

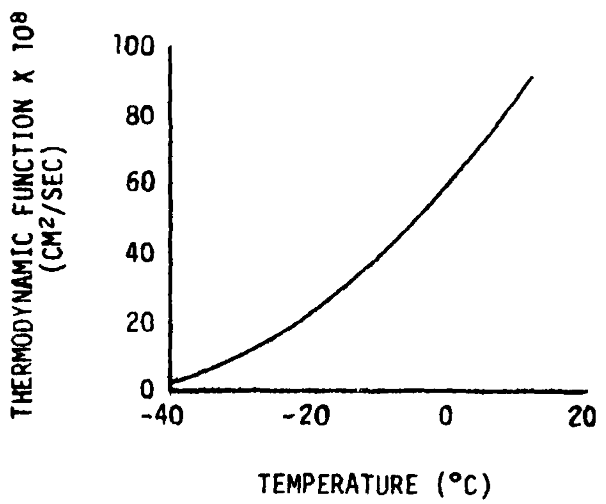

Figure 2. Variation of Thermodynamic Function With Temperature at 1000 Millibars.

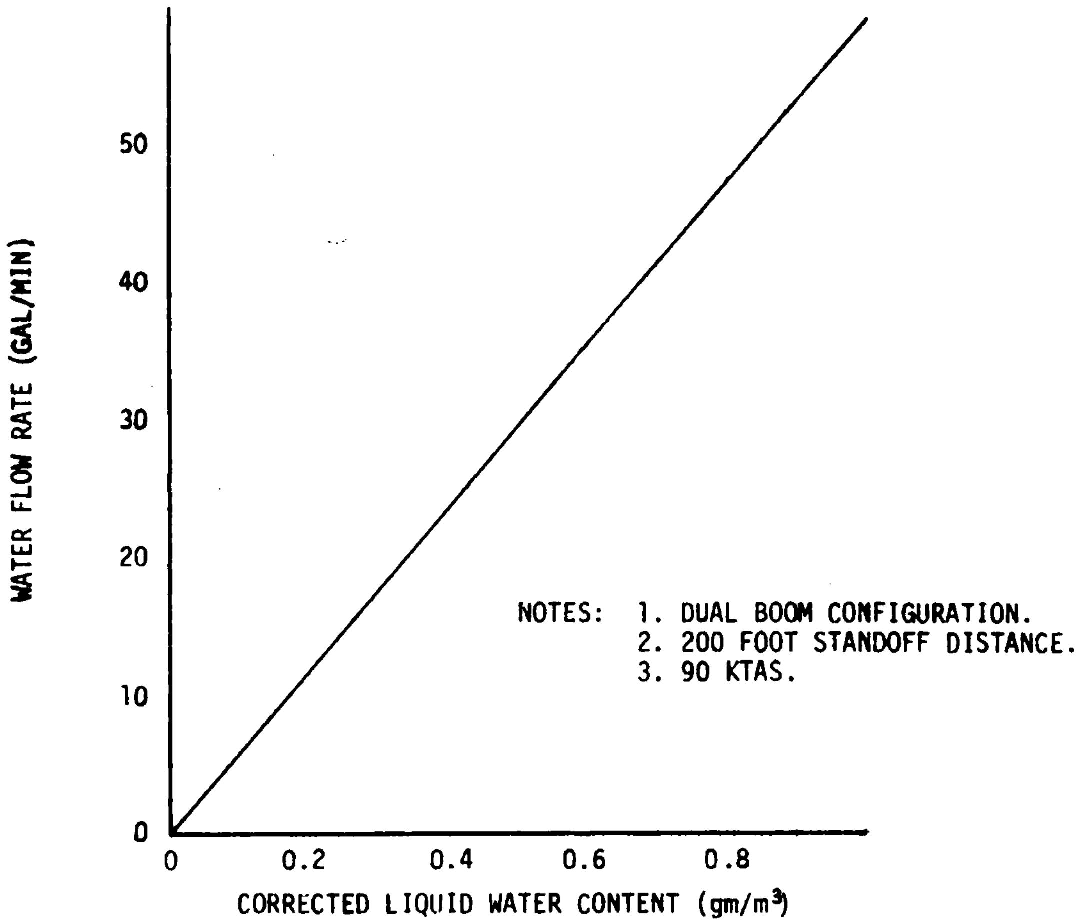

Figure 3. Water Flow Rate Chart - Dual Boom Configuration.

and high-speed photography. Additionally, postflight ice accretions were measured immediately upon landing when practical.

16. Ice shedding characteristics were qualitatively assessed by crewmembers in the test, spray, and chase aircraft. In addition to the high-speed motion pictures taken from the chase and spray aircraft, cameras were mounted on the main and tail rotor blades of the test aircraft. A description of the test aircraft cameras is presented in appendix D. Film obtained from the cameras mounted on the test aircraft did not have sufficient sharpness or clarity to permit an analysis of ice accretion and shedding on the main or tail rotor blades. This was caused by the low ambient light conditions and the unsatisfactory view angles from the location where the cameras were mounted.

17. Vibration levels were qualitatively assessed during each flight. An FM magnetic tape recorder was used to quantify the vibration data. Data obtained from the magnetic tape system were analyzed using a Spectral Dynamics 301 spectral analyzer. The spectral analyzer was used to convert the data from the time domain (acceleration as a function of time) to the frequency domain (acceleration as a function of frequency).

18. Level flight performance degradation due to ice accretion was assessed by comparing the engine power required to maintain constant airspeed and altitude before and after ice accumulation. Shaft horsepower was calculated using equation 4.

$$SHP = N_R \times Q \times K \times \frac{2\pi}{33,000} \tag{4}$$

Where:

SHP = Calculated shaft horsepower (hp)

N_R = Main rotor rotational speed (rev/min)

Q = Engine output shaft torque (ft-lb)

K = Gearing constant between engine and main rotor (76.05)

19. The engine power required to operate the anti-ice/deice systems was also determined by performing engine toppings at various test static air temperatures. The engine topping data were plotted in terms of referred shp versus referred gas temperature ($T_{4.5}$). Referred shp was calculated using equation 5:

$$RSHP = \frac{SHP}{(\delta)(\theta)^{0.5}} \tag{5}$$

Where:

RSHP = Referred shaft horsepower

SHP = Test shaft horsepower

$\delta = 1 - (6.875586 \times 10^{-6})(H_P)^{5.25585}$

H_P = Test pressure altitude (ft)

$$\theta = \frac{OAT_{static} + 273.15}{288.15}$$

OAT_{static} = Test Static air temperature (°C)

20. Autorotational performance degradation due to main and tail rotor ice accretion was evaluated. The collective position required to stabilize at a rotor speed of 276 rpm (105 percent) was measured before and after ice accumulation. The tapeline rates of descent were calculated using equation 6:

$$R/D_{tapeline} = \left(\frac{\Delta H_P}{\Delta t}\right) \frac{T_t}{T_s} \qquad (6)$$

Where:

$R/D_{tapeline}$ = Tapeline rate of descent (ft/min)

$\frac{\Delta H_P}{\Delta t}$ = Change in pressure altitude per given time (ft/min)

T_t = Test ambient air temperature (°K)

T_s = Standard ambient air temperature (°K)

21. The effect of ice accretion on the test aircraft handling qualities was qualitatively assessed by the pilot. An HQRS was used to augment pilot comments and is presented as figure 4. Control positions were quantitatively measured and comparisons made between no-ice base-line data and data recorded after ice accretion.

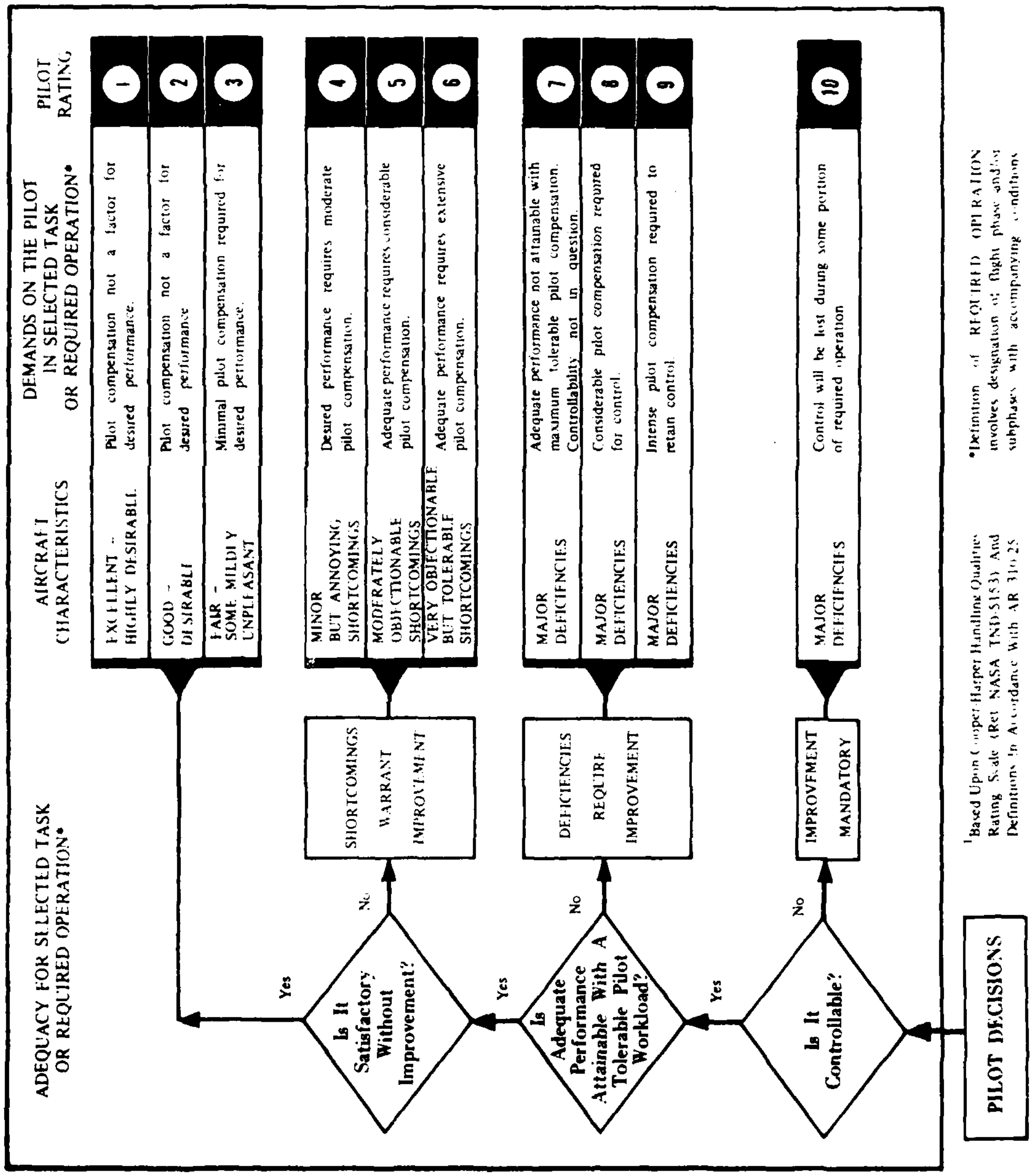

Figure 4. Handling Qualities Rating Scale.

22. Icing characteristics were described using the following definitions of icing types and severity (ref 13, app A).

a. Icing type definitions:

(1) Rime ice: An opaque granular deposit of ice formed by the rapid freezing of small supercooled water droplets.

(2) Clear ice: A semitransparent smooth deposit of ice formed by the slower freezing of larger supercooled water droplets.

(3) Glime ice: A mixture of clear ice and rime ice.

b. Icing severity definitions:

(1) Trace icing: Ice becomes perceptible. Rate of accumulation slightly greater than rate of sublimation. It is not hazardous even though deicing equipment is not used, unless encountered for an extended period of time (over 1 hour).

(2) Light icing: The rate of accumulation may create a problem if flight is prolonged in this environment (over 1 hour). Occasional use of deicing/anti-icing equipment removes/prevents accumulation. It does not present a problem if the deicing/anti-icing equipment is used.

(3) Moderate icing: The rate of accumulation is such that even short encounters become potentially hazardous and use of deicing/anti-icing equipment or diversion is necessary.

(4) Severe icing: The rate of accumulation is such that deicing/anti-icing equipment fails to reduce or control the hazard. Immediate diversion is necessary.

23. Results were categorized as deficiencies or shortcomings in accordance with the following definitions (ref 14, app A):

Deficiency: A defect or malfunction discovered during the life cycle of an equipment that constitutes a safety hazard to personnel; will result in serious damage to the equipment if operation is continued; indicates improper design or other cause of an item or part, which seriously impairs the equipment's operational capability. A deficiency normally disables or immobilizes the equipment; and if occurring during test phases, will serve as a bar to type classification action.

Shortcoming: An imperfection or malfunction occurring during the life cycle of equipment, which should be reported and which must be corrected to increase efficiency and to render the equipment completely serviceable. It will not cause an immediate breakdown, jeopardize safe operation, or materially reduce the usability of the material or end product. If occurring during test phases, the shortcoming should be corrected if it can be done without unduly complicating the item or inducing another undesirable characteristic such as increased cost, weight, etc.

APPENDIX F. ICING FLIGHT SUMMARIES

Table 1. Icing Flight Summary.
Unheated Phase

Flight No. and Date	Average Static Outside Air Temperature (°C)	Programmed Liquid Water Content (gm/m^3)	Average Density Altitude (ft)	Average True Airspeed (kt)	Average Gross Weight (lb)	Average Longitudinal Center of Gravity (in.)
2 12 Oct 76	-11.0	0.25	-340	90	15,600	352.7 (mid)

Time in cloud: (min) Total this flight 5 Cumulative total 5 Number of deice system cycles Zero Type ice observed: Glime

Postflight Ice Measurements (in.)

Component	Maximum Ice	Component	Maximum Ice
Chin bubbles	1/16	Main rotor mast	Trace
Center windshield	1/16	Main rotor hub assembly	Trace
Windshield wipers	1/16	Main rotor pitch change links	Trace
Aircraft nose	1/16	Bifilar	Trace
Eyebrow windows	1/16	Main rotor blades	1/32
Cockpit doors	None	Pitot-static tubes	None
Sponsons	1/16	Engine compartment cooling intakes	1/32
Cockpit door windows	None		
Main landing gear	1/16	FM antenna	Not recorded
Tail gear	None	Horizontal stabilator	Trace
Rotating beacons	None	Vertical fin	Trace
Deice system OAT probe	1/16	Tail rotor hub	None
Ship's system OAT probe	1/16	Tail rotor blades	None
Handholds	None	Hydraulic area fairing	1/16

General comments: 1. Flight objective was to establish OFF time for deice system at test conditions. Test method was to accrete 1/8 inch of ice on main rotor blades or remain in spray cloud for 5 minutes, whichever occurred first.
2. Rosemount and Normalair-Garrett probes were inoperative.
3. Qualitative vibration levels were unchanged.
4. Chase observer indicated rotor disc was only partially immersed in spray cloud.
5. Engine torque increased 7 percent to maintain trim level flight after immersion.

FOR OFFICIAL USE ONLY

Table 2. Icing Flight Summary.
Unheated Phase

Flight No. and Date	Average Static Outside Air Temperature (°C)	Programmed Liquid Water Content (gm/m^3)	Average Density Altitude (ft)	Average True Airspeed (kt)	Average Gross Weight (lb)	Average Longitudinal Center of Gravity (in.)
3 13 Oct 76	-5.5	0.25	2880	90	15,700	353.1 (mid)

Time in cloud: (min)	Total this flight 10 Cumulative total 15	Number of deice system cycles Zero	Type ice observed: Glime

Postflight Ice Measurements (in.)

Component	Maximum Ice	Component	Maximum Ice
Chin bubbles	1/16	Main rotor mast	1/16
Center windshield	3/32	Main rotor hub assembly	1/16
Windshield wipers	3/8	Main rotor pitch change links	1/4
Aircraft nose	1/16	Bifilar	1/8
Eyebrow windows	1/16	Main rotor blades	3/16
Cockpit doors	1/16	Pitot-static tubes	None
Sponsens	1/16	Engine compartment cooling intakes	3/16
Cockpit door windows	1/16	FM antenna	1/16
Main landing gear	3/32	Horizontal stabilator	1/8
Tail gear	None	Vertical fin	1/32
Rotating beacons	Trace	Tail rotor hub	None
Deice system OAT probe	1/16	Tail rotor blades	None
Ship's system OAT probe	1/4	Hydraulic area fairing	1/16
Handholds	1/8		

General comments: 1. Flight objective was to establish the OFF time for deice system for the test conditions.
2. Pilot windshield wiper failed approximately 8 minutes after entering the cloud.
3. No change in vibration levels was noted.
4. Engine torque increased 3 percent to maintain trim level flight after immersion.
5. No ice was observed to shed in flight. Ice was shed at the landing site.

Table 3. Icing Flight Summary.
Heated Phase

Flight No. and Date	Average Static Outside Air Temperature (°C)	Programmed Liquid Water Content (gm/m3)	Average Density Altitude (ft)	Average True Airspeed (kt)	Average Gross Weight (lb)	Average Longitudinal Center of Gravity (in.)
6 18 Oct 76	-6.0	0.25	5380	88	15,900	353.9 (mid)

Time in cloud: (min) Total this flight 16 Cumulative total 31 Number of deice system cycles 4 Type ice observed: Glime

Postflight Ice Measurements (in.)

Component	Maximum Ice	Component	Maximum Ice
Chin bubbles	1/16	Main rotor mast	1/16
Center windshield	1/8	Main rotor hub assembly	1/16
Windshield wipers	3/16	Main rotor pitch change links	1/16
Aircraft nose	1/8	Bifilar	3/16
Eyebrow windows	1/16	Main rotor blades	1/8
Cockpit doors	1/16	Pitot-static tubes	None
Sponsons	None	Engine compartment cooling intakes	5/16
Cockpit door windows	1/16	FM antenna	1/4
Main landing gear	None	Horizontal stabilator	1/16
Tail gear	None	Vertical fin	None
Rotating beacons	None	Tail rotor hub	1/16
Deice system OAT probe	1/16	Tail rotor blades	None
Ship's system OAT probe	3/16	Hydraulic area fairing	Trace
Handholds	Not recorded		

General comments: 1. Flight objective was to establish ON time for the deice system. Test method was to enter cloud for 4 minutes, accrete ice, exit cloud, turn deice system until blade surface temperatures reached +5°C. This was repeated to optimize ON time. Then the system was turned on in the cloud to check its operation.
2. A main rotor 4/rev increase in the vertical axis was noted at the pilot seat.
3. Engine torque increased 11 percent to maintain trim level flight after the last immersion.

FOR OFFICIAL USE ONLY

Table 4. Icing Flight Summary.
Heated Phase

Flight No. and Date	Average Static Outside Air Temperature (°C)	Programmed Liquid Water Content (gm/m^3)	Average Density Altitude (ft)	Average True Airspeed (kt)	Average Gross Weight (lb)	Average Longitudinal Center of Gravity (in.)
8 19 Oct 76	-5.5	0.25	8960	89	16,100	354.8 (mid)

Time in cloud: (min) **Total this flight** 21 **Cumulative total** 52 **Number of deice system cycles** 8 **Type ice observed: Glime**

Postflight Ice Measurements (in.)

Component	Maximum Ice	Component	Maximum Ice
Chin bubbles	1/8	Main rotor mast	3/16
Center windshield	1/8	Main rotor hub assembly	Not recorded
Windshield wipers	Not recorded	Main rotor pitch change links	1/8
Aircraft nose	1/8	Bifilar	1/8
Eyebrow windows	1/8[5]	Main rotor blades	5/16
Cockpit doors	None[5]	Pitot-static tubes	None
Sponsens	1/8[5]	Engine compartment cooling intakes	3/8
Cockpit door windows	None[5]	FM antenna	Not recorded
Main landing gear	None[5]	Horizontal stabilator	1/8
Tail gear	None[5]	Vertical fin	1/16
Rotating beacons	None[5]	Tail rotor hub	None
Deice system OAT probe	3/16	Tail rotor blades	None
Ship's system OAT probe	3/16	Hydraulic area fairing	Not recorded
Handholds	1/8[5]		

General comments: 1. Objective of test was to remain in cloud until an aircraft limitation was reached.
2. The aircraft did not have sufficient power to maintain flight in the spray cloud at this altitude. Flight was aborted since there were no alternative test conditions available. The deice system was functioning properly.
3. Engine torque increased 6 percent to maintain trim level flight after the first attempt to remain in the cloud.

FOR OFFICIAL USE ONLY

Table 5. Icing Flight Summary.
Heated Phase

Flight No. and Date	Average Static Outside Air Temperature (°C)	Programmed Liquid Water Content (gm/m^3)	Average Density Altitude (ft)	Average True Airspeed (kt)	Average Gross Weight (lb)	Average Longitudinal Center of Gravity (in.)
13 28 Oct 76	-10.5	0.25	450	90	15,560	357.2 (mid)

Time in cloud: (min) **Total this flight** 8 **Cumulative total** 60 **Number of deice system cycles** 2 **Type ice observed: Glime**

Postflight Ice Measurements (in.)

Component	Maximum Ice	Component	Maximum Ice
Chin bubbles	1/16	Main rotor mast	1/16
Center windshield	1/16	Main rotor hub assembly	1/16
Windshield wipers	1/8	Main rotor pitch change links	1/8
Aircraft nose	1/16	Bifilar	1/8
Eyebrow windows	Trace	Main rotor blades	1/4
Cockpit doors	1/8	Pitot-static tubes	None
Sponsens	Trace	Engine compartment cooling intakes	1/4
Cockpit door windows	None	FM antenna	1/8
Main landing gear	None	Horizontal stabilator	1/32
Tail gear	None	Vertical fin	1/16
Rotating beacons	Trace	Tail rotor hub	None
Deice system OAT probe	1/16	Tail rotor blades	Trace
Ship's system OAT probe	1/8	Hydraulic area fairing	1/32
Handholds	1/8		

General comments: 1. Flight objective was to check deice system operation in the spray cloud.
2. Pilot windshield wiper failed just after entering the cloud.
3. Main rotor blades shed symmetrically when deice system was activated.
4. Rosemount probe was inoperative.
5. Engine torque increased 15 percent to maintain trimmed level flight after immersion.
6. Maximum steady-state autorotational rotor speed was degraded to 97 percent from 105 percent after cloud immersion. Collective was in the full-down position.

Table 6. Icing Flight Summary.
Heated Phase

Flight No. and Date	Average Static Outside Air Temperature (°C)	Programmed Liquid Water Content (gm/m^3)	Average Density Altitude (ft)	Average True Airspeed (kt)	Average Gross Weight (lb)	Average Longitudinal Center of Gravity (in.)
14 29 Oct 76	-12.0	0.25	1140	92	14,860	354.1 (mid)

Time in cloud: (min)	Total this flight 53 Cumulative total 113	Number of deice system cycles 12	Type ice observed: Glime

Postflight Ice Measurements (in.)

Component	Maximum Ice	Component	Maximum Ice
Chin bubbles	3/16	Main rotor mast	3/8
Center windshield	5/16	Main rotor hub assembly	1/4
Windshield wipers	5/16	Main rotor pitch change links	1/4
Aircraft nose	5/16	Bifilar	1/4
Eyebrow windows	1/2	Main rotor blades	5/8
Cockpit doors	Trace	Pitot-static tubes	None
Sponsens	1/2	Engine compartment cooling intakes	1-1/4
Cockpit door windows	1/8		
Main landing gear	Not recorded	FM antenna	1
Tail gear	Not recorded	Horizontal stabilator	1/2
Rotating beacons	Not recorded	Vertical fin	1/4
Deice system OAT probe	3/4	Tail rotor hub	Trace
Ship's system OAT probe	3/8	Tail rotor blades	1/4
Handholds	7/8	Hydraulic area fairing	3/16

General comments: 1. Objective of test was to remain in the cloud until an aircraft limitation was reached.
2. Deice system functioned normally. Ice was shed after each cycle.
3. Slight increase in main rotor 4/rev in the lateral axis was noted during flight in the cloud. Vibration was noted to reduce after each heating cycle was complete.
4. Engine torque increased 12 percent to maintain trim level flight after immersion.
5. Maximum steady-state autorotational rotor speed was degraded to 95 percent from 105 percent after cloud immersion. Collective was in the full-down position.
6. Significant amounts of ice (up to 1-1/2 inches) accreted forward of eyebrow window from runback of windshield wipers.

FOR OFFICIAL USE ONLY

Table 7. Icing Flight Summary.
Unheated Phase

Flight No. and Date	Average Static Outside Air Temperature (°C)	Programmed Liquid Water Content (gm/m^3)	Average Density Altitude (ft)	Average True Airspeed (kt)	Average Gross Weight (lb)	Average Longitudinal Center of Gravity (in.)
15 30 Oct 76	-12.0	0.50	720	90	15,180	355.4 (mid)

Time in cloud: (min)	**Total this flight** 4 **Cumulative total** 117	**Number of deice system cycles** Zero	**Type ice observed: Glime**

Postflight Ice Measurements (in.)

Component	Maximum Ice	Component	Maximum Ice
Chin bubbles	1/8	Main rotor mast	1/16
Center windshield	1/8	Main rotor hub assembly	1/16
Windshield wipers	1/8	Main rotor pitch change links	3/16
Aircraft nose	1/16	Bifilar	1/8
Eyebrow windows	1/8	Main rotor blades	3/16
Cockpit doors	3/16	Pitot-static tubes	1/8
Sponsons	1/8	Engine compartment cooling intakes	1/8
Cockpit door windows	None	FM antenna	1/4
Main landing gear	Not recorded	Horizontal stabilator	3/32
Tail gear	Not recorded	Vertical fin	Trace
Rotating beacons	Trace	Tail rotor hub	Trace
Deice system OAT probe	1/8	Tail rotor blades	Trace
Ship's system OAT probe	1/8	Hydraulic area fairing	1/8
Handholds	Not recorded		

General comments: 1. Test objective was to determine the deice system OFF time for test conditions. Test method was to accrete 1/8 inch of ice on main rotor blades or remain in the cloud for 4 minutes, whichever occurred first.
2. No change in vibration levels was observed.
3. Engine torque increased 21 percent to maintain trim level flight after the cloud immersion.
4. Engine compartment fire extinguisher tube (No. 2 engine) accreted 1/8 inch ice. Nozzle was not blocked.
5. Runback behind pitot-static mount was noted.

Table 8. Icing Flight Summary.
Heated Phase

Flight No. and Date	Average Static Outside Air Temperature (°C)	Programmed Liquid Water Content (gm/m^3)	Average Density Altitude (ft)	Average True Airspeed (kt)	Average Gross Weight (lb)	Average Longitudinal Center of Gravity (in.)
16 1 Nov 76	-15.0	0.25	-1060	93	14,980	354.7 (mid)

Time in cloud: (min) **Total this flight** 16 **Cumulative total** 133

Number of deice system cycles 4

Type ice observed: Glime

Postflight Ice Measurements (in.)

Component	Maximum Ice	Component	Maximum Ice
Chin bubbles	1/8	Main rotor mast	3/16
Center windshield	1/4	Main rotor hub assembly	1/8
Windshield wipers	3/8	Main rotor pitch change links	5/16
Aircraft nose	3/16	Bifilar	3/16
Eyebrow windows	1/4	Main rotor blades	3/16
Cockpit doors	1/4	Pitot-static tubes	1/4
Sponsens	3/8	Engine compartment cooling intakes	5/8
Cockpit door windows	None	FM antenna	5/8
Main landing gear	Not recorded	Horizontal stabilator	1/8
Tail gear	Not recorded	Vertical fin	1/16
Rotating beacons	Trace	Tail rotor hub	Not recorded
Deice system OAT probe	Not recorded	Tail rotor blades	Not recorded
Ship's system OAT probe	Not recorded	Hydraulic area fairing	Not recorded
Handholds	Not recorded		

General comments: 1. Test objective was to remain in cloud until an aircraft limitation was reached.
2. An object from the HISS was observed to go through the test helicopter rotor disc. Flight was aborted.
3. Engine torque increased 13 percent to maintain trim level flight after cloud immersion.
4. Rotor blades had ice remaining on heated blade areas. It was found that the potentiometer settings on the deice system were incorrect.
5. Contractor icing rate probe iced up. Broken electrical wire.

Table 9. Icing Flight Summary.
Heated Phase

Flight No. and Date	Average Static Outside Air Temperature (°C)	Programmed Liquid Water Content (gm/m^3)	Average Density Altitude (ft)	Average True Airspeed (kt)	Average Gross Weight (lb)	Average Longitudinal Center of Gravity (in.)
17 2 Nov 76	-11.0	0.50	-820	88	15,180	355.4 (mid)

Time in cloud: (min) **Total this flight** 34 **Cumulative total** 167 **Number of deice system cycles** 10 **Type ice observed: Glime**

Postflight Ice Measurements (in.)

Component	Maximum Ice	Component	Maximum Ice
Chin bubbles	5/8	Main rotor mast	3/4
Center windshield	3/4	Main rotor hub assembly	1/2
Windshield wipers	2	Main rotor pitch change links	7/8
Aircraft nose	3/8	Bifilar	1/2
Eyebrow windows	Trace	Main rotor blades (unheated area)	1
Cockpit doors	3/4	Pitot-static tubes (mount)	1-1/2
Sponsens	3/4	Engine compartment cooling intakes	2
Cockpit door windows	1/4	FM antenna	5/8
Main landing gear	1	Horizontal stabilator	3/8
Tail gear	1/8	Vertical fin	3/8
Rotating beacons	1	Tail rotor hub	1/16
Deice system OAT probe	1-1/16	Tail rotor blades	1/8
Ship's system OAT probe	1-1/4	Hydraulic area fairing	1/2
Handholds	1-1/2		

General comments: 1. Test objective was to remain in the cloud until an aircraft limitation was reached.
2. Vibration levels were observed to increase slightly during flight in the cloud.
3. A rotor speed excursion was accomplished during flight in the cloud and additional ice was shed.
4. Engine torque increased 20 percent to maintain trim level flight after the cloud immersion.
5. A second rotor speed excursion was accomplished after exiting the cloud and additional ice was shed from the inboard sections of the main rotor. The engine torque required to maintain trim level flight also decreased to 4 percent above that required before icing.
6. The maximum steady-state autorotational rotor speed was degraded to 97 percent with collective in the full-down position from 104 percent, with 7 percent collective control remaining.
7. During the autorotation the stabilator failed due to the disturbed airflow around the ice accreted above the windshields, causing the airspeed sensors to fluctuate.

Table 10. Icing Flight Summary.
Heated Phase

Flight No. and Date	Average Static Outside Air Temperature (°C)	Programmed Liquid Water Content (gm/m^3)	Average Density Altitude (ft)	Average True Airspeed (kt)	Average Gross Weight (lb)	Average Longitudinal Center of Gravity (in.)
19 3 Nov 76	-16.0	0.25	-840	90	15,440	356.7 (mid)

Time in cloud: (min) Total this flight 42 Cumulative total 209 Number of deice system cycles 9 Type ice observed: Glime

Postflight Ice Measurements (in.)

Component	Maximum Ice	Component	Maximum Ice
Chin bubbles	3/16	Main rotor mast	9/16
Center windshield	1/4	Main rotor hub assembly	1/2
Windshield wipers	1	Main rotor pitch change links	7/8
Aircraft nose	1/4	Bifilar	1/2
Eyebrow windows	3/4	Main rotor blades	7/8
Cockpit doors	Trace	Pitot-static tubes (mount)	1/4
Sponsens	1/2	Engine compartment cooling intakes	2
Cockpit door windows	Not recorded	FM antenna	1-1/8
Main landing gear	3/4	Horizontal stabilator	Not recorded
Tail gear	Not recorded	Vertical fin	Not recorded
Rotating beacons	1/4	Tail rotor hub	Not recorded
Deice system OAT probe	5/8	Tail rotor blades	Not recorded
Ship's system OAT probe	11/16	Hydraulic area fairing	Not recorded
Handholds	Not recorded		

General comments: 1. Test objective was to remain in the cloud until an aircraft limitation was reached.
2. An asymmetrical ice loading developed after a rotor speed excursion was used in an attempt to shed ice on the inboard section of the main rotor. Cockpit vibration levels of the main rotor 1/rev increased to 0.12g (measured on the on-board Chadwick-Helimuth meter).
3. Engine torque increased 11 percent to maintain trim level flight after immersion.
4. The maximum steady-state autorotational rotor speed was degraded to 103 percent with the collective control in the full-down position from 104 percent with 7 percent collective control remaining.
5. A rotor speed excursion was accomplished after the postcloud performance data were obtained but was not effective in reducing the engine power required to maintain trim level flight. No additional ice was shed.

FOR OFFICIAL USE ONLY

APPENDIX G. TEST DATA

INDEX

FIGURE 1

REFERRED ENGINE OUTPUT SHAFT HORSEPOWER AND REFERRED MEASURED GAS TEMPERATURE

AIRCRAFT YUH-60A S/N 73-21651 ENGINE YT700-GE-700 S/N 207267 (LEFT)

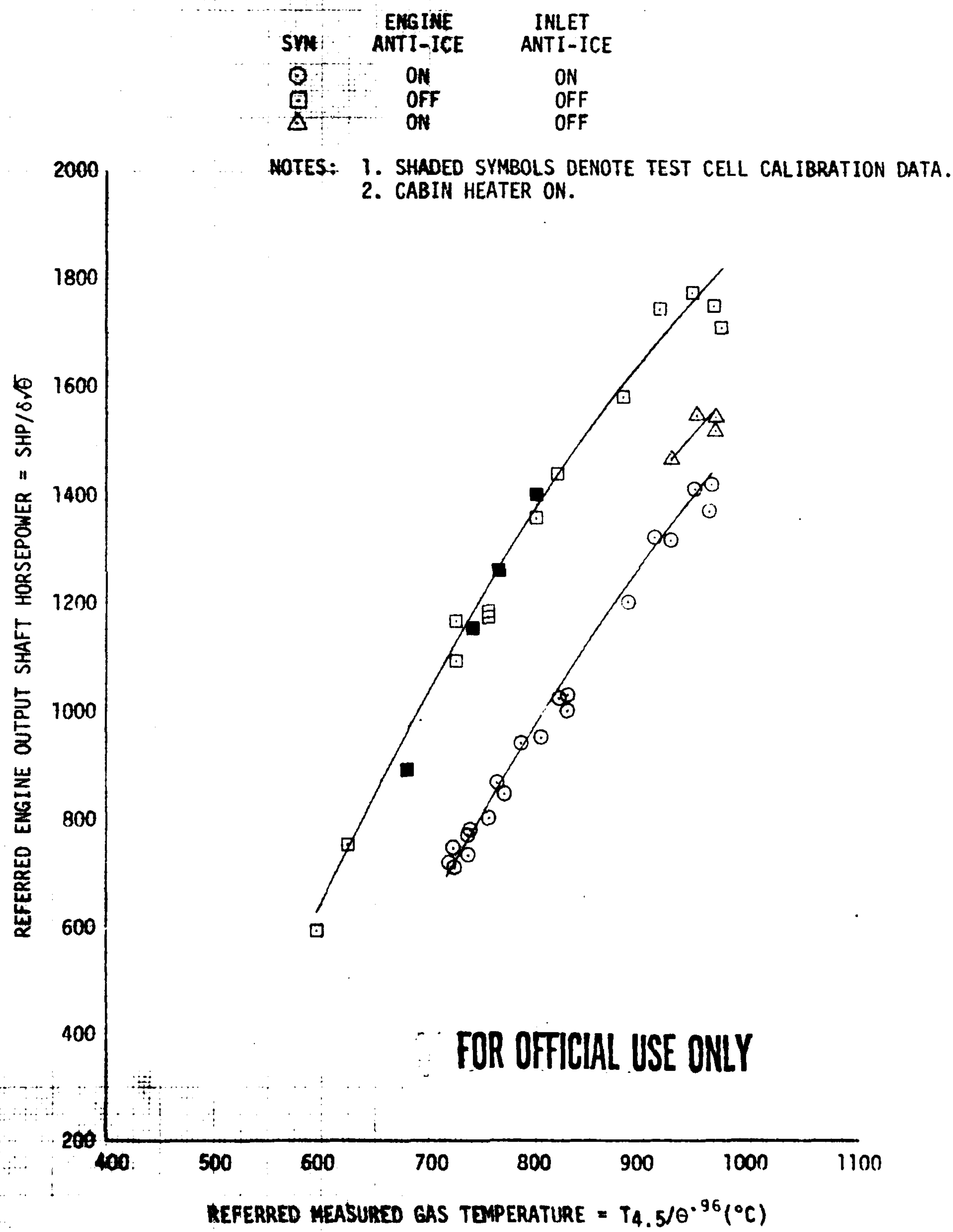

FIGURE 2

REFERRED ENGINE OUTPUT SHAFT HORSEPOWER AND REFERRED MEASURED GAS TEMPERATURE

AIRCRAFT YUH-60A S/N 73-21651 ENGINE YT700-GE-700 S/N 207268 (RIGHT)

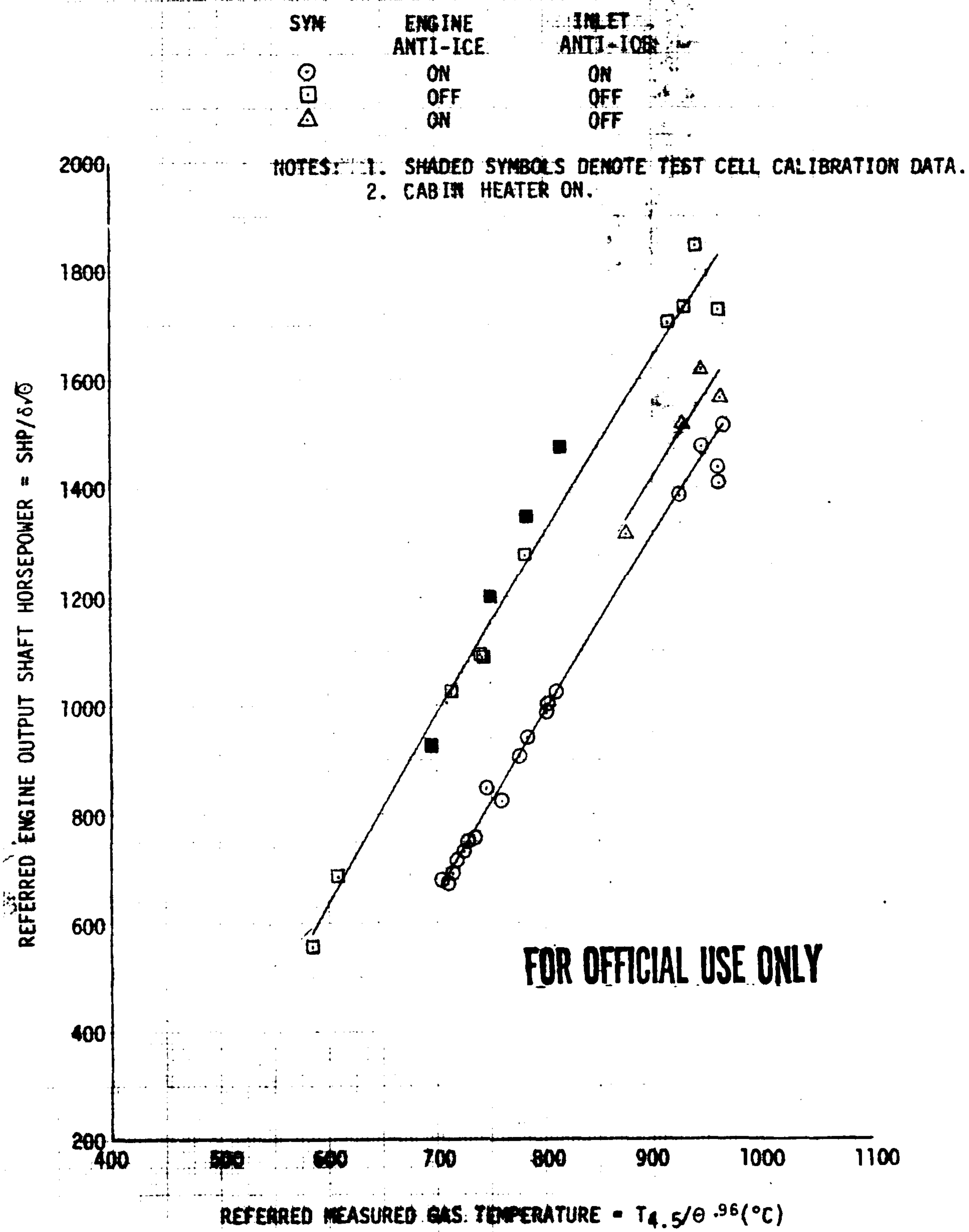

FIGURE 3

VIBRATION CHARACTERISTICS

YUH-60A USA S/N 73-21651

LOCATION: PILOT SEAT

AXIS: LATERAL

FUNDAMENTAL FREQUENCY IS 4.30 HZ

GROSS WEIGHT -LB	LONG CG FS -IN.	LAT CG BL -IN.	DENSITY ALTITUDE -FT	OUTSIDE AIR TEMPERATURE -DEG C	ROTOR SPEED -RPM	TRIM CALIB. AIRSPEED -KTS	FLIGHT CONDITION	CONFIGURATION
15440	357	0	-840	-16.0	258	90	LEVEL	NORMAL UTILITY

NOTE: DATA OBTAINED PRIOR TO ENTRY INTO ICING CLOUD.

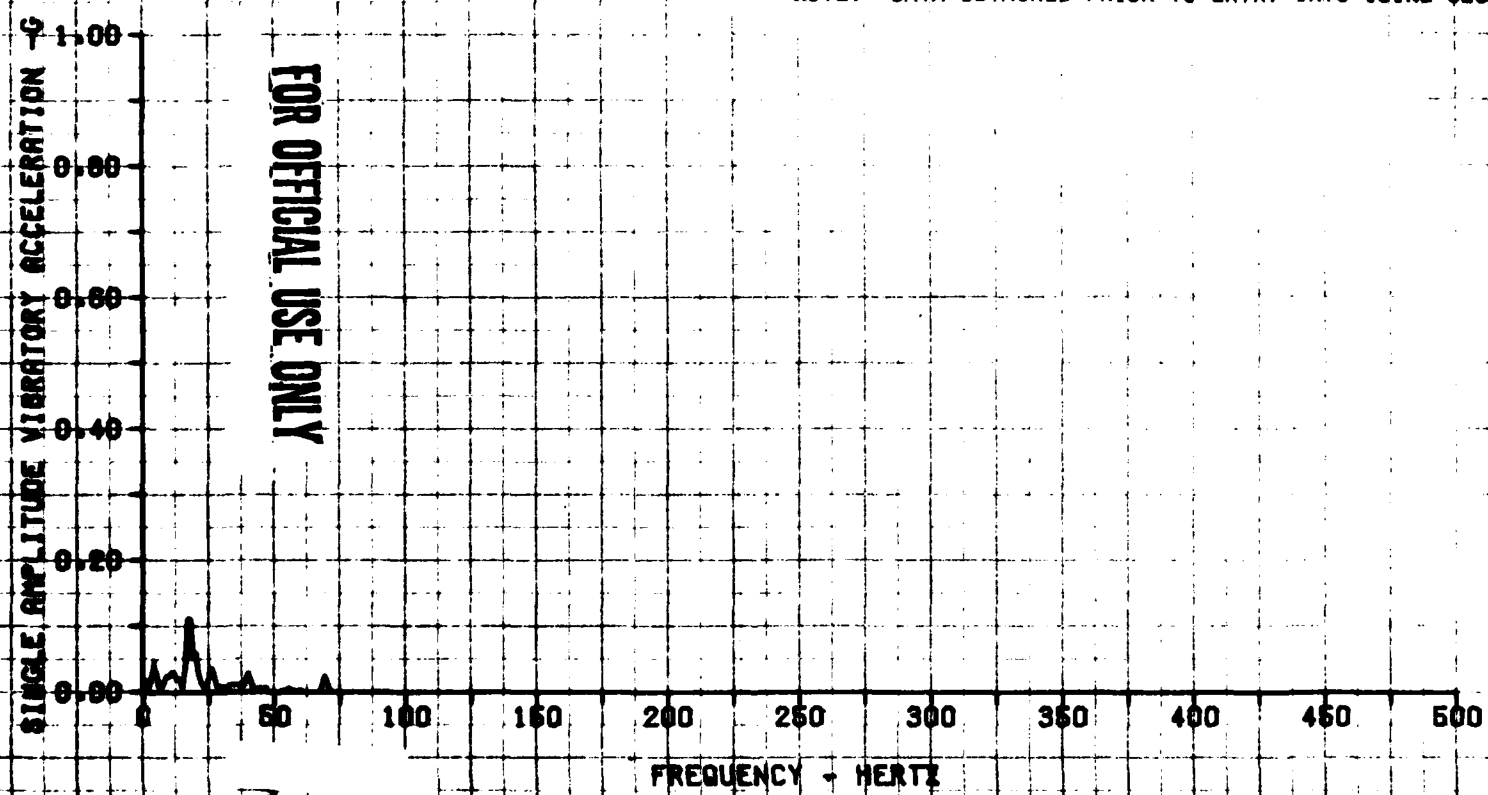

FOR OFFICIAL USE ONLY

FIGURE 4

VIBRATION CHARACTERISTICS

YUH-60A USA S/N 73-21651

LOCATION: PILOT SEAT

FUNDAMENTAL FREQUENCY IS 4.30 HZ

AXIS LATERAL

GROSS WEIGHT -LB	LONG CG FS -IN.	LAT CG BL -IN.	DENSITY ALTITUDE -FT	OUTSIDE AIR TEMPERATURE -DEG C	ROTOR SPEED -RPM	TRIM CALIB. AIRSPEED -KTS	FLIGHT CONDITION	CONFIGURATION
15440	357	0	-840	-16.0	258	90	LEVEL	NORMAL UTILITY

NOTE: DATA OBTAINED WITH AN ASYMMETRICAL ICE LOADING ON THE MAIN ROTOR.

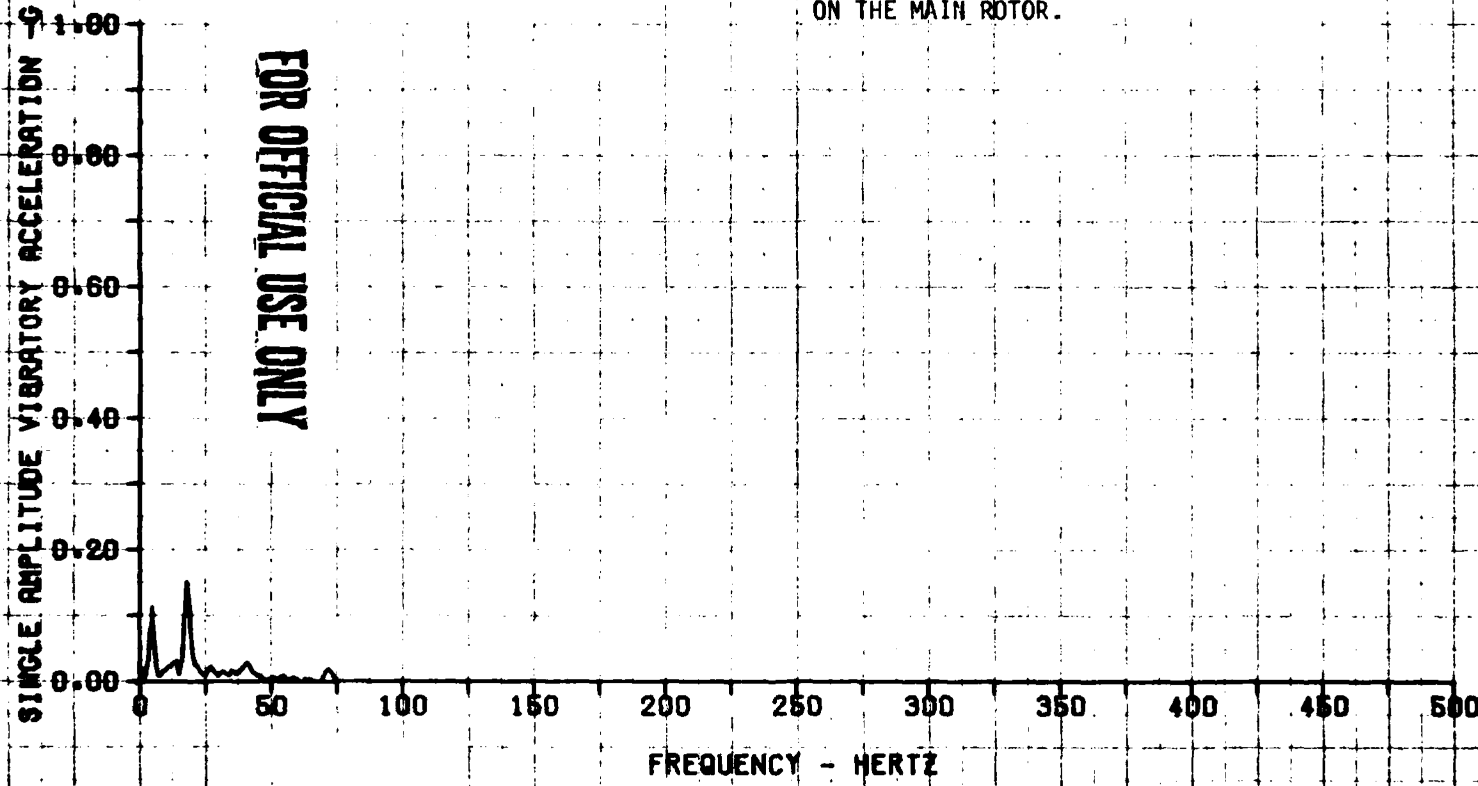

FOR OFFICIAL USE ONLY

86

APPENDIX H. PHOTOGRAPHS

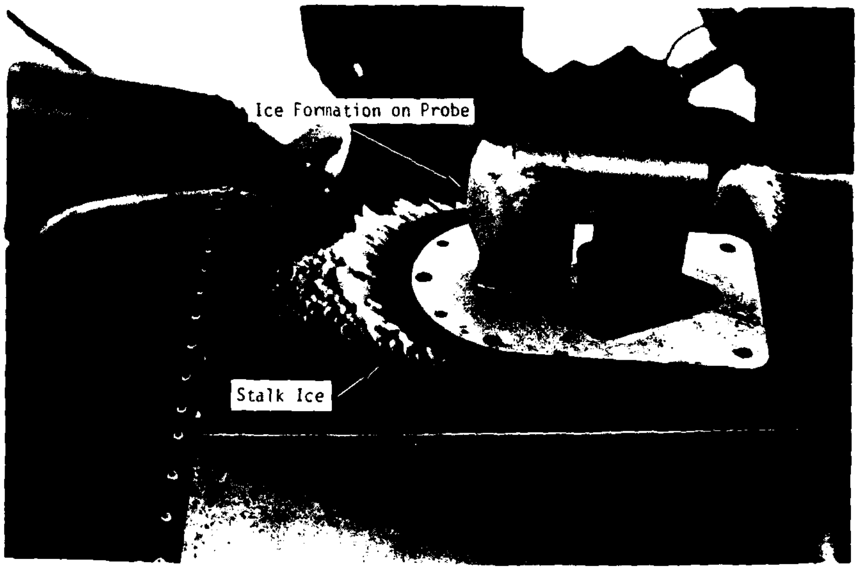

Photo 1. Aspirated Rosemount 851F Icing Rate Detector After Flight 16.

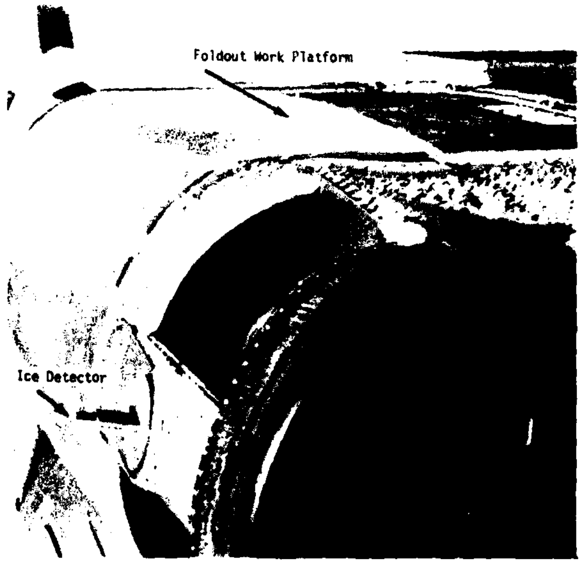

Photo 2. Rosemount 851F Icing Rate Detector Location.

~~FOR OFFICIAL USE ONLY~~

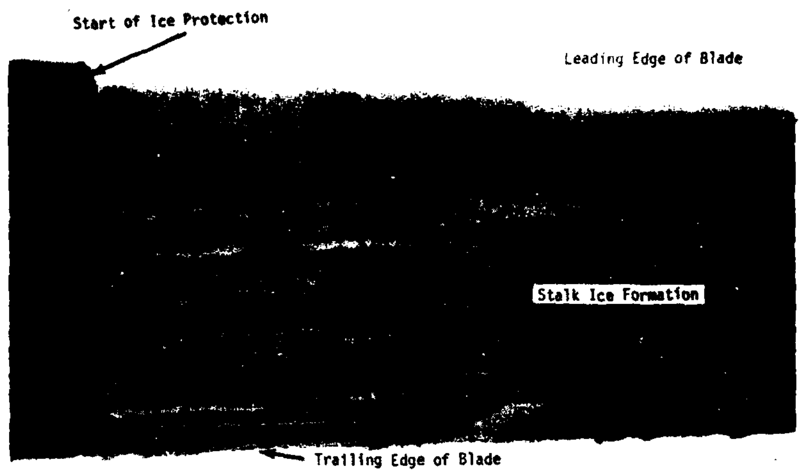

Photo 3. "Stalk" Ice Remaining on Bottom Side of Main Rotor Blade

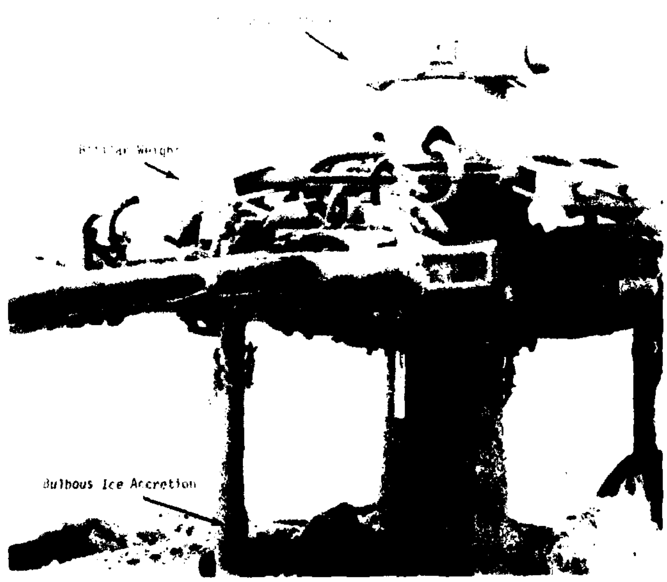

Photo 4. Main Rotor Hub Area After Flight 19.

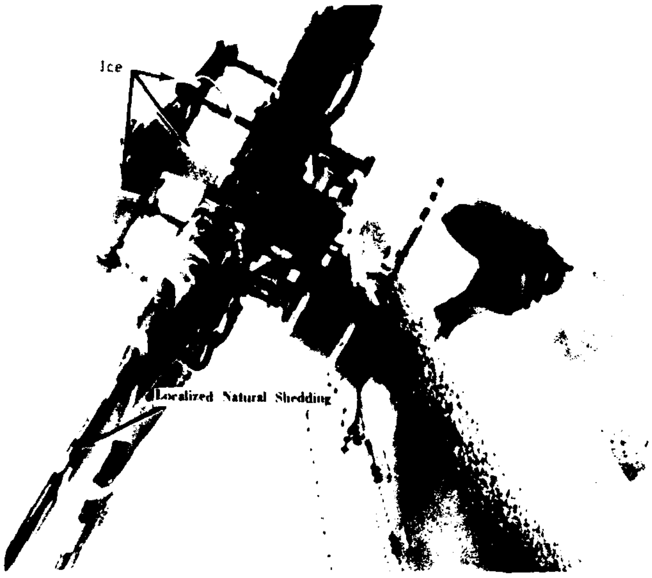

Photo 5. Tail Rotor Blades and Tail Rotor Gearbox Fairing After Flight 19.

Photo 6. Ice Accretion on Aircraft During Flight 17.

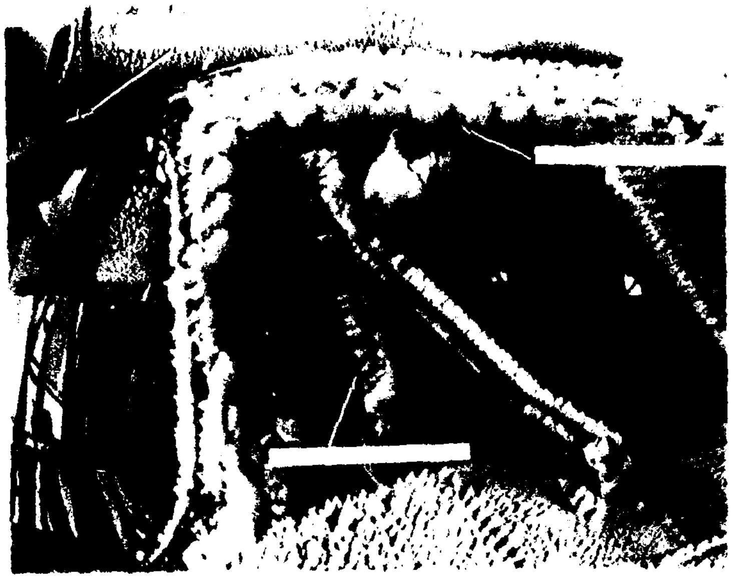

Photo 7. Ice Accretion on Pilot's Windshield Flight 17.

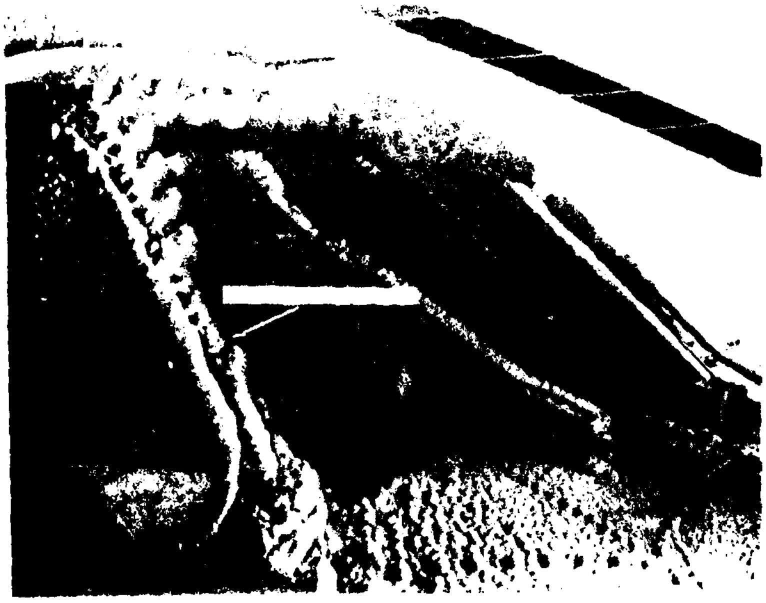

Photo 8. Ice Accretion on Pilot's Door, Flight 17.

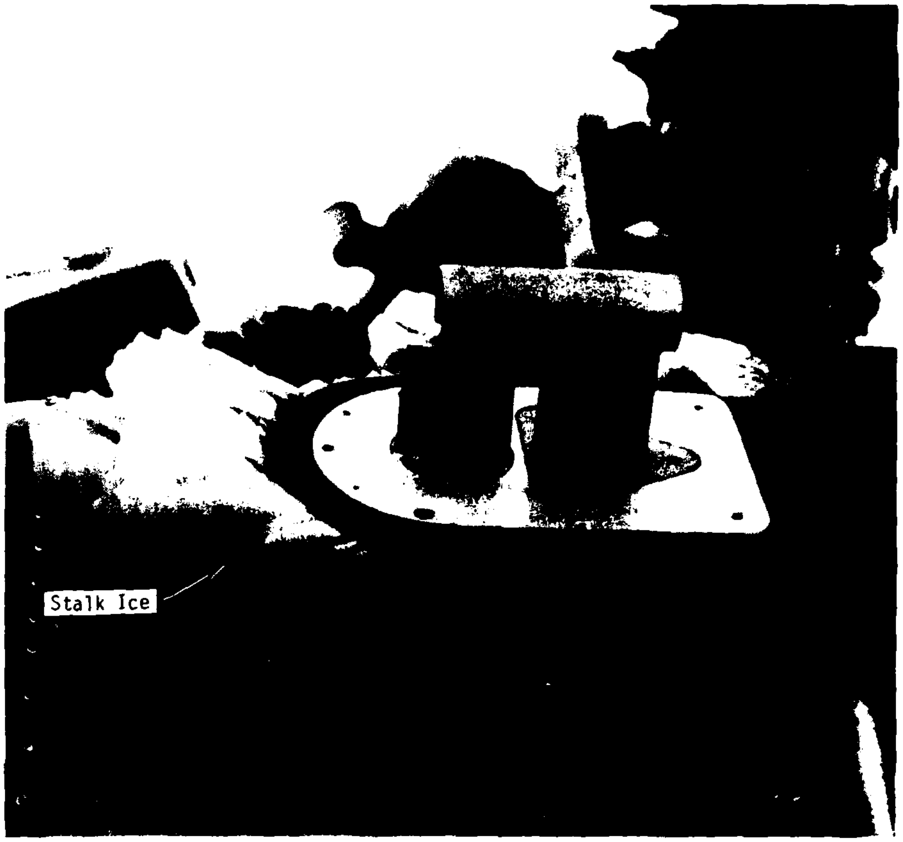

Photo 9. Ice Accretion on Front of Aspirated Rosemount 851F

DISTRIBUTION

Director of Defense Research and Engineering	2
Assistant Secretary of the Army (R&D)	1
Deputy Chief of Staff for Research, Development, and Acquisition (DAMA-WSA, DAMA-RA, DAMA-PPM-T)	4
US Army Materiel Development and Readiness Command (DRCPM-UA, DRCSF-A, DRCQA, DRCPM-TND-AV)	9
US Army Aviation Systems Command (DRSAV-EQ, DRSAV-EX)	14
US Army Training and Doctrine Command (ATCD-TM, ATCD-CM-C)	2
US Army Test and Evaluation Command (DRSTE-AV)	3
Hq US Army Air Mobility R&D Laboratory (SAVDL-D)	2
US Army Air Mobility R&D Laboratory (SAVDL-SR)	1
Ames Directorate, US Army Air Mobility R&D Laboratory (SAVDL-AM)	2
Eustis Directorate, US Army Air Mobility R&D Laboratory (SAVDL-EU-SY)	1
Langley Directorate, US Army Air Mobility R&D Laboratory (SAVDL-LA)	2
US Army Aeromedical Research Laboratory (SGRD-UAC)	1
US Army Aviation Center (ATZQ-D-M)	1
US Army Infantry School (ATSH-CD-UG)	1
US Army Aviation Board (ATZQ-OT-CM)	1
US Army Aircraft Development Test Activity (STEBG-PD-P)	5
US Army Agency for Aviation Safety (IGAR-TA, IGAR-Library)	2
US Army Operational Test and Evaluation Agency (CSTE TM-AV)	3
US Army Materiel Systems Analysis Activity (DRXSY-CM)	2
US Army Transportation School (ATSP-CD-MS)	1
US Naval Air Systems Command (PMA-266, Air 5104)	3
US Naval Air Test Center (RW 60)	3
Sikorsky Aircraft Division of United Technologies Corporation	5
General Electric Company, Aircraft Engine Group	5
Defense Documentation Center	2

DATE
FILMED

2-8